Neurobiology of Disease

Maternal Immune Activation during Pregnancy Alters Postnatal Brain Growth and Cognitive Development in Nonhuman Primate Offspring

Roza M. Vlasova,[1*] Ana-Maria Iosif,[2*] Amy M. Ryan,[3,4,5*] Lucy H. Funk,[3] Takeshi Murai,[5] Shuai Chen,[2] Tyler A. Lesh,[3] Douglas J. Rowland,[6] Jeffrey Bennett,[3] Casey E. Hogrefe,[5] Richard J. Maddock,[3] Michael J. Gandal,[7] Daniel H. Geschwind,[7] Cynthia M. Schumann,[3,4] Judy Van de Water,[4,8] A. Kimberley McAllister,[4,9] Cameron S. Carter,[3] Martin A. Styner,[1,10] David G. Amaral,[3,4,5] and Melissa D. Bauman[3,4,5]

[1]Department of Psychiatry, University of North Carolina, Chapel Hill, North Carolina, 27514, [2]Division of Biostatistics, Department of Public Health Sciences, School of Medicine, University of California, Davis, Sacramento, California, 95817, [3]Department of Psychiatry and Behavioral Sciences, School of Medicine, University of California, Davis, Sacramento, California, 95817, [4]The MIND Institute, School of Medicine, University of California, Davis, Sacramento, California, 95817, [5]California National Primate Research Center, University of California, Davis, California, 95616, [6]Center for Genomic and Molecular Imaging, University of California, Davis, California, 95616, [7]Neurogenetics Program, Department of Neurology, University of California, Los Angeles, California, 90095, [8]Rheumatology/Allergy and Clinical Immunology, School of Medicine, University of California, Davis, Sacramento, California, 95817, [9]Center for Neuroscience, University of California, Davis, California, 95618, and [10]Department of Computer Science, University of North Carolina, Chapel Hill, North Carolina, 27599

Human epidemiological studies implicate exposure to infection during gestation in the etiology of neurodevelopmental disorders. Animal models of maternal immune activation (MIA) have identified the maternal immune response as the critical link between maternal infection and aberrant offspring brain and behavior development. Here we evaluate neurodevelopment of male rhesus monkeys (*Macaca mulatta*) born to MIA-treated dams ($n = 14$) injected with a modified form of the viral mimic polyinosinic:polycytidylic acid at the end of the first trimester. Control dams received saline injections at the same gestational time points ($n = 10$) or were untreated ($n = 4$). MIA-treated dams exhibited a strong immune response as indexed by transient increases in sickness behavior, temperature, and inflammatory cytokines. Although offspring born to control or MIA-treated dams did not differ on measures of physical growth and early developmental milestones, the MIA-treated animals exhibited subtle changes in cognitive development and deviated from species-typical brain growth trajectories. Longitudinal MRI revealed significant gray matter volume reductions in the prefrontal and frontal cortices of MIA-treated offspring at 6 months that persisted through the final time point at 45 months along with smaller frontal white matter volumes in MIA-treated animals at 36 and 45 months. These findings provide the first evidence of early postnatal changes in brain development in MIA-exposed nonhuman primates and establish a translationally relevant model system to explore the neurodevelopmental trajectory of risk associated with prenatal immune challenge from birth through late adolescence.

Key words: animal model; autism; MRI; neuroimmunology; rhesus monkey; schizophrenia

Significance Statement

Women exposed to infection during pregnancy have an increased risk of giving birth to a child who will later be diagnosed with a neurodevelopmental disorder. Preclinical maternal immune activation (MIA) models have demonstrated that the effects of maternal infection on fetal brain development are mediated by maternal immune response. Since the majority of MIA models are conducted in rodents, the nonhuman primate provides a unique system to evaluate the MIA hypothesis in a species closely related to humans. Here we report the first longitudinal study conducted in a nonhuman primate MIA model. MIA-exposed offspring demonstrate subtle changes in cognitive development paired with marked reductions in frontal gray and white matter, further supporting the association between prenatal immune challenge and alterations in offspring neurodevelopment.

Introduction

The current COVID-19 pandemic highlights an urgent need to understand the association between maternal infection during pregnancy and the subsequent increased risk of offspring neurodevelopmental disorders (NDDs). Although the long-term effects of prenatal SARS-CoV-2 exposure are unknown, converging epidemiological data suggest that, for a subset of women, infections during pregnancy are associated with an increased risk of NDDs in their offspring, including both schizophrenia (SZ) and autism spectrum disorder (ASD) (Estes and McAllister, 2016; Keôpińska et al., 2020). The diversity of viral and bacterial pathogens associated with NDDs suggests that maternal immune response is the critical link between maternal infection and altered fetal neurodevelopment (Knuesel et al., 2014). Moreover, the presence of inflammatory biomarkers in gestational biospecimens lends further support to the association between maternal immune activation (MIA) and risk of offspring NDDs (Brown and Meyer, 2018). Even in the absence of an NDD diagnosis, emerging evidence from human studies links variation in maternal cytokine levels during pregnancy with various offspring neurobehavioral outcomes, including alterations in brain growth, functional connectivity, and behavioral and cognitive development (Schepanski et al., 2018). Collectively, these studies suggest that changes in maternal cytokines during pregnancy can have long-lasting consequences, ranging from subtle differences in brain and behavioral development to severe NDDs.

The preclinical MIA model has emerged as a powerful translational tool that allows investigators to manipulate maternal cytokine levels during gestation and systematically evaluate offspring neurodevelopmental consequences in a controlled environment. MIA models use immune activating agents, such as the viral mimic polyinosinic:polycytidylic acid (Poly IC), to elicit an immune response during gestation. Across species, offspring of MIA-treated dams exhibit alterations in brain and behavioral development relevant to human neurodevelopmental and neuropsychiatric disease, supporting the initial interpretation of the MIA model as an animal model of ASD or SZ (Meyer and Feldon, 2010; Careaga et al., 2017). As preclinical research evolves toward a hypothesis-based approach (Gordon, 2019), cross-species MIA model comparisons in mice, rats, and nonhuman primates (NHPs) provide new opportunities to maximize the translational utility of this promising animal model and to explore neurobiological mechanisms underlying human NDDs (Kentner et al., 2019). Similarities in placental structure and physiology, gestational timelines, brain development, neuroanatomical organization, and behavioral complexity between humans and NHPs (Bauman and Schumann, 2018; Testard et al., 2021) provide a unique opportunity to evaluate the foundational knowledge of the rodent MIA model in a species more closely related to humans.

Our research team developed the first Poly IC-based NHP model to explore the neurodevelopmental trajectory of risk associated with prenatal immune challenge in the rhesus monkey (*Macaca mulatta*). In our previous study, pregnant rhesus monkeys injected with a modified form of Poly IC at the end of the first or second trimester exhibited a transient but potent immune response and produced offspring that deviated from species-typical behavioral development (Bauman et al., 2014; Machado et al., 2015; Rose et al., 2017). Although *in vivo* imaging and postmortem brain tissue studies were limited in these initial NHP MIA cohorts, the emergence of atypical behaviors as the animals matured suggested that this model system may provide an opportunity to explore circuitry relevant to NDDs that may be vulnerable to prenatal immune challenge. Indeed, these small cohorts of MIA-treated NHPs demonstrated increased striatal dopamine in late adolescence as indexed by PET (Bauman et al., 2019), aberrant dendritic morphology in the DLPFC (Weir et al., 2015), and region-specific alterations in gene expression (Page et al., 2021). We have generated a larger cohort of late first trimester MIA-treated male offspring to perform a comprehensive evaluation of brain and behavioral development from birth to late adolescence to characterize the emergence of brain and behavioral alterations in MIA-exposed NHPs. Here we present our initial findings of longitudinal structural MRI and cognitive performance data from this unique NHP MIA model.

Materials and Methods

All experimental procedures were developed in collaboration with the veterinary, animal husbandry, and environmental enrichment staff at the California National Primate Research Center (CNPRC) and approved by the University of California, Davis Institutional Animal Care and Use Committee. All attempts were made (in terms of social housing, enriched diet, use of positive reinforcement strategies, and minimizing the duration of daily training/testing sessions) to promote normal social development and psychological well-being of the animals that participated in this research. Gestational timing, choice of species, source of immune activating agent, and subsequent magnitude of the MIA determine the impact on offspring neurodevelopment in preclinical MIA models. In accordance to recent guideline recommendations for improving the reporting of MIA model methods, we have completed the reporting table from Kentner et al. (2019) and will be provided upon request.

Animal selection

Pregnant dams were selected from the indoor, time-mated breeding colony based on age, weight, parity, and number of prior live births (Table 1). Candidate dams between 5 and 12 years old carrying a male fetus were assigned to MIA ($n = 14$) or control/saline ($n = 10$). Because of limited availability of male fetuses, untreated pregnant females confirmed to be carrying male fetuses were added to the control group ($n = 4$). One offspring from the MIA group was killed at 6 months of age because of

Table 1. Summary of dam characteristics[a]

Dam characteristic	MIA (n = 14)	Control (n = 10 saline, n = 4 untreated)
Age at conception (yr)	9.2 (2.4)	8.7 (2.2)
Weight at GD 40 (kg)	7.5 (1.5)	7.7 (1.6)
Prior conceptions	4.7 (2.0)	3.6 (2.2)

[a] Data are mean (Standard deviation, SD).

an unrelated health condition and is not included in behavior or neuroimaging datasets after 6 months of age. A second animal from the MIA-treated group was killed at 42 months because of an unrelated health condition and is not included in the final neuroimaging time point.

MIA and validation
MIA induction protocols are based on our previous dosing and gestational timing experiments previously described (Bauman et al., 2014, 2019; Machado et al., 2015; Weir et al., 2015). Synthetic double-stranded RNA (Poly IC stabilized with poly-L-lysine [Poly ICLC]; Oncovir; 0.25 mg/kg i.v.) or sterile saline (equivalent volume to Poly ICLC) was injected at 07:30 h in the cephalic vein in awake animals on gestational day (GD) 43, 44, and 46 (Table 2). Health and behavior observations were conducted 3 times before treatment, 6 h after each of the three injections, and 3 times after treatment. The checklist captured the presence or absence of any clinical or behavioral symptoms resulting from the infusions, including change in appetite, watery eyes or nasal discharge, liquid stool, lethargy or labored movements, and body temperature. Before infusions, programmable temperature microchips (Bio Medic Temperature Systems) were implanted subcutaneously under sedation near the left and right clavicle, and a temperature wand then scanned the microchip and displayed body temperature. Temperatures were recorded just before Poly ICLC or saline injection, and 30 min, 6 h, and 8 h after injection. Pretreatment and posttreatment baseline temperatures were taken during health and behavior observations. Blood was collected from the dams on approximately GD 40 while sedated for ultrasound (pretreatment), from awake animals on GD 44 and 46, 6 h after Poly ICLC infusion, and on GD 51 or 52 while sedated for a recheck ultrasound (posttreatment) for cytokine analysis. Blood samples were centrifuged and the serum was removed, aliquoted into 200 μl samples, and frozen at −80°C until analysis. A longitudinal analysis on the maternal IL-6 response to Poly ICLC exposure was measured in serum using an NHP multiplexing bead immunoassay (MilliporeSigma) that was analyzed using the flow-based Luminex 100 suspension array system (Bio-Plex 200; Bio-Rad Laboratories). Hair samples were collected from the dams at GD 150 to evaluate potential group differences in chronic stress during pregnancy.

Hair cortisol analysis
Hair samples were collected from the dams at GD 150 when they were sedated for an ultrasound by shaving the nape of the neck. Samples were then placed in tubes and stored in a −80°C freezer. Samples were not collected from 3 of the untreated controls, resulting in Control (n = 11) and MIA (n = 14). Cortisol concentrations were analyzed using established protocols (Vandeleest et al., 2019) by extracting cortisol from hair using methanol and then measured using a salivary cortisol kit (Salimetrics). Intra-assay coefficient of variability was 1.6%.

Rearing conditions and husbandry
Infants were raised in individual cages with their mothers where they had visual access to other mother-infant pairs at all times. For 3 h each day, one familiar adult male and four familiar mother-infant pairs were allowed to freely interact in a large cage (3 m [length] × 1.8 m [width] × 2 m [height]) to provide enrichment and facilitate species-typical social development. The rearing groups consisted of two MIA-treated mother-infant dyads and two control mother-infant dyads. Dominance hierarchies naturally formed between the dams, and group stability was monitored throughout by trained observers. The infants were weaned from their mothers at 6 months of age and were permanently paired with a familiar peer from their rearing group. Weanlings continued the same

socialization routine through ~18 months of age. They were transferred to the large enclosures for 3 h each day with the same three weanlings from their rearing group, the familiar adult male, and an adult female who was not one of the dams involved in the study. Animal rooms were maintained at 18°C-29°C and on a 12/12 light/dark cycle (lights on at 06:00). Subjects were fed twice daily (Lab Diet #5047, PMI Nutrition International), and provided with forage scratch daily and fresh produce biweekly; they had access to water *ad libitum* along with a variety of enrichment devices.

Offspring physical growth, neurodevelopmental milestones, and early behavioral development
Measures of body growth (weight, crown-rump length, and head circumference) were collected at 1 and 3 months of age as well as at the neuroimaging time points (6, 12, 24, 36, and 45 months of age). The NHP offspring described in this paper underwent comprehensive assessments of social development that will be the focus of future publications. Here data are presented on a neurobehavioral neonatal assessment conducted at 1 week of age, home cage observations of the mother-infant dyad (0-6 months), and home cage observations with their age/sex/treatment-matched cage mate (6-18 months) (Table 3). All behavioral observations were conducted by trained observers demonstrating an interobserver reliability > 85% (agreements/[agreements + disagreements] × 100). Each infant received a dye mark, allowing the observers to record behaviors while remaining blind to their experimental condition. Detailed methods are provided in previous publications (Bauman et al. 2004a,b, 2013, 2014).

Neonatal assessment. The development of reflexes and basic neuromotor functioning was assessed at 7 (±1) days of age. The dam was lightly sedated with ketamine to remove the infant, and the infant was transferred to a testing room. A 5 point scale of maturity was used to rate the infant on measures of visual orientation and the following: reflexes including rooting, righting, placing, and Moro; motor maturity including head posture, coordination of movements, and prone progression; and state control (agitation and consolability). For each assessment, infants were given a score as follows: 2, present/fully developed; 1.5, mostly present/developed; 1, partially present or partially developed; 0.5, slightly developed or present; or 0, absent.

Mother-infant home cage observation (0-6 months). Each mother-infant dyad was observed 5 d per week in the home cage by a trained observer who was familiar to the animals yet blinded to the condition of the animals. Interactions were quantified using a checklist of behaviors to describe the type and frequency of interactions between the mother and infant. Behaviors included nursing, grooming, contact, maternal behaviors (restrain, retrieve, rejection, aggression), facial expressions, environmental exploration, and stereotypy. Observations were conducted between 08:00 and 15:00 and continued until weaning at ~6 months of age. The 1 min observation was broken into six 10 s bins, and one-zero sampling was used to record behaviors. In one-zero sampling, every behavior that is present within each bin receives a score of 1 regardless of the number of times it occurs within the bin. Behaviors that are absent within each bin receive a score of 0.

Infant-infant home cage observations (6-18 months). Each infant-infant dyad was observed 3 d/wk for 52 weeks in the home cage by a trained observer who was familiar to the animals yet blinded to the condition of the animals. Interactions were quantified using a checklist of behaviors to describe the type and frequency of interactions between familiar peers. Behaviors included sleep, nonsocial activity, proximity, contact, play, environmental exploration, and stereotypy. Observations were conducted between 08:00 and 15:00 beginning 1 week after the dyads were formed at weaning at ~6 months of age. The 1 min observation was scored in six 10 s bins as described above.

Cognitive assessments
Reversal learning (RL). RL paradigms are used across a range of species, including humans, and entail assessing cognitive flexibility in animals when reward outcomes for stimuli are reversed (Izquierdo and Jentsch, 2012). Training began at 19.5 months to displace a single gray cube placed in the left, right, or center position on the Wisconsin

Table 2. Maternal response to poly ICLC

GD	Poly ICLC Injection	Temperature	Appetite	Cytokine
Baseline (minimum 24 h before first injection)	—	Baseline temperature	1:30 PM Three assessments across 10 d	8:00 AM Baseline blood draw
GD 43	7:30 AM Injection 1	7:30 AM 8:00 AM 1:30 PM 3:30 PM	1:30 PM	—
GD 44	7:30 AM Injection 2	7:30 AM 8:00 AM 1:30 PM 3:30 PM	1:30 PM	1:30 PM Blood drawn 6 h after injection 2
GD 45	No injection	—	—	—
GD 46	7:30 AM Injection 3	7:30 AM 8:00 AM 1:30 PM 3:30 PM	1:30 PM	1:30 PM Blood drawn 6 h after injection 3
Baseline (minimum 96 h after last injection)	—	Baseline temperature	1:30 PM Three assessments across 10 d	8:00 AM Baseline blood draw

Table 3. Home cage interaction behavioral ethogram

Behavior	Description
Maternal contact (pre-wean only)	
Breast contact	Focal infant suckles mother
Ventral contact	Ventral surface of the focal contacts ventral surface of dam
Other contact	Other physical contact (not breast contact or ventral contact) with dam
No contact	No physical contact between infant and dam
Maternal interaction (pre-wean only)	
Maternal restrain	Mother physically interferes with the infant's attempts to move away from her
Maternal retrieve	Mother physically brings infant closer to her
Maternal reject	Mother physically prevents the focal infant from contact
Exploratory events (composite score)	
Toy play	Oral or manual manipulation of toys in cage
Oral explore	Oral manipulation to any part of the cage, excluding food
Manual explore	Manual manipulation to any part of the cage
Total stereotypies (composite score)	
Pace	Repetitive undirected pacing with the same path repeated at least 3 consecutive times
Head twist	Throwing of the head back and to the side in an exaggerated manner
Backflip	Repetitive backflip at least two times in a row
Bounce	Repetitive bounce up and down at least two times in a row
Nipple clasp	Holding of the nipple
Rock	Stationary rocking either back and forth or side to side
Swing	Swinging within the cage for at least 3 s
Self-bite	Biting motion of own limb or body part
Salute	Fingers or hand held in place along the brow, eyes, or other part of the upper face
Other abnormal behavior	Any other abnormal behaviors not described above
Infant-infant interaction (post-wean only)	
Nonsocial activity	Not in proximity, contact, play or other social activity
Home cage proximity	Both animals are in the same cage
Contact	Any physical contact between the focal animal and another
Play	Any instance of play (contact play, wrestle play, chase)

General Testing Apparatus (WGTA) within a 30 s timeframe to reveal a reward underneath. Monkeys were transported to the testing room in a modified transport box that when secured enabled them to reach out through a Plexiglas panel and fully participate with the WGTA. Each daily training session consisted of 20 trials, and training continued until a criterion of 18 of 20 retrievals in a session. Weekly maintenance training sessions were conducted until testing began at 21 months of age. For the RL assessment, monkeys were tested in 20 daily sessions using two identical cubes differing only in color (black and white). The cubes were placed to the right and left of center on the WGTA test board. The black cube was initially designated correct, and when displaced, revealed a food reward in the well underneath. The well covered by the white cube did not contain a food reward. Right/left placement of the correct cube followed a random order for the 20 trials per session. Daily testing continued until the monkeys performed 18 of 20 trials correct in a session. Once this criterion was reached, the reward contingencies were reversed in the next testing session (the white cube was correct and the black cube was incorrect). When the 18 of 20 criterion was reached, the contingencies were again reversed. The number of reversal events monkeys were able to achieve within 20 sessions were measured. Response latency on each trial was also recorded as well as a rating of the monkey's temperament during the session. For temperament, the experimenter who tested the monkey rated its temperament shortly after the completion of the testing session. Monkeys were rated on a 0-3 scale on object orientation, goal directivity, irritability, activity, inhibition, impulsivity, stereotypies, attention to the task, and its behavior during omission errors.

Automated cognitive testing. Automated cognitive testing via computerized touchscreen devices allowed more complex assessments during the older juvenile stage. The remaining cognitive tests were conducted with the Cambridge Neuropsychological Test Automated Batteries software (CANTAB, Cambridge Cognition) on a modified desktop computer, touchscreen, and automated reward dispenser using protocols for rhesus monkeys (Weed et al., 1999; Golub et al., 2005, 2014, 2017). Sugar pellets (Bio-Serv) were used for rewards. Animals were tested in their home cage and temporarily separated in place from their partner. Testing occurred between 07:30 and 11:30, and the morning meal was fed following testing. *Ad libitum* access to water was available throughout testing. Touchscreen training using successive approximation began between 32 and 33 months of age as previously described (Golub et al., 2017). All monkeys then passed the box training module criteria of 10 consecutive box touches within 10 min for 2 consecutive sessions.

Continuous performance task (CPT). Sustained attention and response inhibition were assessed at 33-34 months of age via the CPT module on the CANTAB apparatus. CPT was designed as a go/no-go task in which three different colored boxes were presented one at a time on the screen. White boxes were correct and rewarded with a sugar pellet
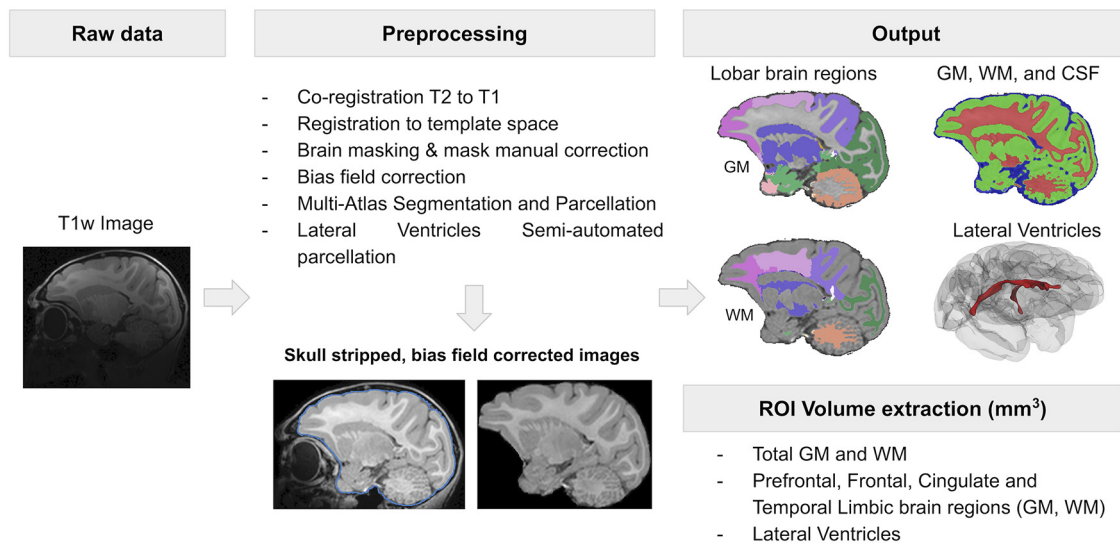
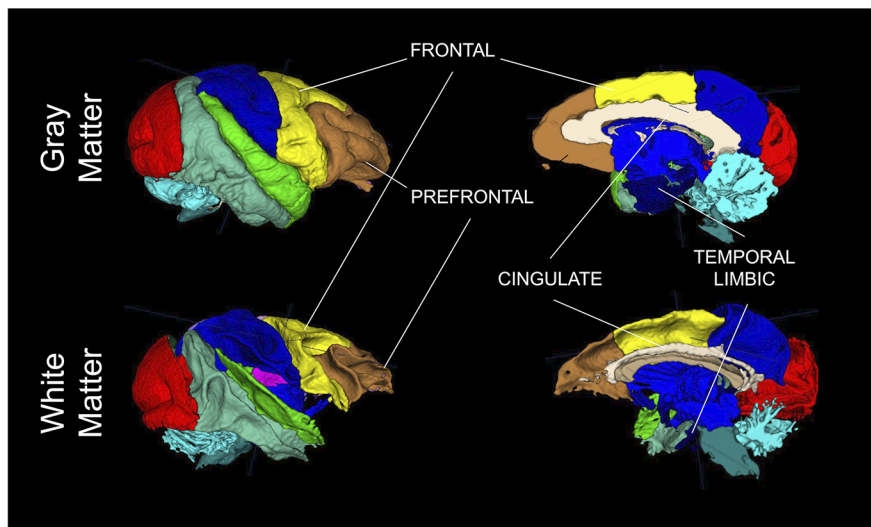**Figure 1.** Structural MRI analysis workflow.

Figure 2. ROI visualization.

when touched. Red and green boxes were incorrect and were not rewarded when touched. Equal numbers of the three colored boxes were presented for 3 s each across 84 trials in one daily 10 min testing session. Correct responses were thus selecting the white box and not selecting, or inhibiting a response, to the red and green boxes. Incorrect responses were failing to select the white box or selecting the red or green boxes and resulted in a longer intertrial interval (3 s blank screen timeout). Monkeys had two attempts to touch a white box 5 times within 30 s to initiate their daily testing session and ultimately had 30 testing sessions. Performance was assessed for hits (correct responses), misses (omission errors), correct rejections (not selecting an incorrect box), false alarms (selecting an incorrect box), and signal detection theory measures of response accuracy (d'), nonresponse bias, and response bias (β).

Progressive ratio break point task (PRBT). Motivation with respect to reward efficacy was tested with the Progressive Ratio CANTAB task. Monkeys began testing at 40-41 months of age and had 10 daily sessions. For this task, they had to touch a blue rectangle to retrieve a food reward, and the number of touches increased geometrically every 8 trials over the testing session. For example, the monkeys had to touch the box once for a reward for the first 8 trials, but then two touches for the next 8 trials, four touches for the following 8 trials, 8 touches for next 8 trials, etc. Daily sessions lasted for 30 min or until 3 min passed since a box was last

touched. The progressive break point was considered the point at which the animal stopped responding and the session ended.

Probabilistic RL (PRL). A more complex RL paradigm was introduced at 44-45 months of age. PRL is the RL test usually conducted in humans because it reduces the possibility that individuals develop a simple win-stay lose-shift strategy instead of continuing to acquire information on each trial. In this CANTAB module, two stimuli did not have a binary yes/no reward contingency as they did in the WGTA RL task, but rather, one stimulus was more likely, but not guaranteed, to be rewarded instead of the other stimulus. To begin, a basic RL task with 100% reward probability (one stimulus always correct and one stimulus always incorrect) was used to establish consistent performance on the computerized task. Each 30 min daily testing session consisted of 60 trials, a 30 s stimulus presentation length, 5 s intertrial interval, and 5 s darkness timeout following incorrect responses. When the monkeys reached 90% (54 of 60) correct in a session, the PRL paradigm began the next day with two new stimuli. In this paradigm, there was a 90:10 reward ratio where one stimulus was rewarded 90% of the time and the other stimulus was rewarded 10% of the time. Thus, 10% of the time, the reward contingency was possibly unexpected based on what the monkeys learned about the reward outcomes for each stimulus. When a monkey achieved 85% (51 of 60) correct for the session, the reward contingencies for the stimuli were reversed in the next testing session. With the same pair of stimuli, the one that was previously rewarded 90% of the time was now rewarded 10% of the time, and vice versa. As with the RL paradigm in the WGTA, the number of reversal events monkeys were able to achieve within 20 sessions was assessed.

Intradimensional/extradimensional (ID/ED) shift. The ID/ED task is a computerized adaptation of the Wisconsin Card Sorting Task and is designed to test cognitive flexibility with respect to being able to shift from a learned set of rules to another, or attentional set shifting. Monkeys were 46-47 months old and began this task 2 d after completion of PRL. The premise of ID/ED was that the monkeys were presented with two stimuli and they learned the rule for the correct/rewarded one, and when a criterion was reached, the rule for which stimulus to select changed. There were four stages to the ID/ED task. Each stage consisted

Table 4. Maternal IL-6 response

	MIA (n = 14)		Control (n = 10)	
	Mean (SD)	Median [range]	Mean (SD)	Median [range]
Il-6 (pg/ml)				
Pre-dosing (GD 40)	10.9 (28.7)	0.9 [0.0-108.3]	0.6 (0.6)	0.4 [0.0-1.8]
After second injection (GD 44)	777.9 (1068.6)	450.9 [90.8-4341.7]	4.6 (9.6)	1.0 [0.0-31.4]
After third injection (GD 46)	493.0 (751.4)	130.4 [51.7-2780.7]	6.8 (18.6)	0.4 [0.0-59.5]
Il-6 change from baseline (pg/ml)				
After second injection (GD 44)	767.3 (1072.9)	450.9 [89.1-4341.7]	4.0 (9.4)	0.6 [−0.7 to 30.4]
After third injection (GD 46)	482.3 (754.0)	129.8 [50.0-2777.7]	6.2 (18.6)	0.0 [−0.2 to 59.1]

Table 5. Descriptive statistics for appetite changes during poly ICLC injections[a]

	MIA (n = 14)		Control (n = 10)	
Time	Mean (SD)	Median [range]	Mean (SD)	Median [range]
Pretreatment[b]	1.1 (0.7)	1.3 [0-2]	1.5 (0.4)	1.5 [0.7-2]
Treatment	0.4 (0.4)	0.3 [0-1.3]	1.6 (0.4)	1.7 [0.7-2]
Post-treatment[c]	1.3 (0.5)	1.3 [0.3-2]	1.3 (0.5)	1.3 [0.3-2]

[a]Pretreatment = 3 d between GD 32 and 42; Treatment = GD 43, 44, and 46; Post-treatment = 3 d between GD 47 and 57. Appetite was rated on a 0-2 Likert-type scale as follows: 0 = poor (1-3 biscuits eaten); 1 = fair (4-6 biscuits eaten); 2 = good (7-9 biscuits eaten). For each period, scores were first summarized within-animal, by calculating the average over 3 d.
[b]All 3 d missing data for 1 animal in MIA group.
[c]One day missing data for 1 animal in MIA group.

of a rewarded stimulus acquisition and then reversal of rewarded stimulus. The first stage was a simple discrimination in which two stimuli of different shapes were presented. One shape was rewarded until a criterion of 12 correct responses out of the last 15 trials was reached. On the subsequent trial, the previously rewarded stimulus became incorrect and the previously incorrect stimulus became correct (simple discrimination reversal [SDR]). When the criterion (12 of 15) was reached in the reversal round, the task moved to the second stage. This was the compound discrimination stage, in which the same shape stimuli from Stage 1 were used and had the same reward contingencies as the reversal round, but the stimuli now had lines superimposed on them to create compound stimuli. The monkeys had to learn to select the previously rewarded shape no matter which of the two lines was superimposed on it in each trial. As with Stage 1, the rewarded stimulus was then reversed after the monkey reached criterion (compound discrimination reversal [CDR]). Following criterion on Stage 2, the task moved to Stage 3, the ID. In this stage, two new shape and line stimuli were presented, yet the same relevant dimension of shape was rewarded. The monkeys had to learn both the dimension and stimulus to select for a reward. Once criterion was reached, the other shape stimulus was rewarded for the reversal round (ID shift reversal). After criterion was reached for both rounds of the third stage, the fourth stage was the ED. Two new shape and line stimuli were presented, but now it was the line stimuli that were relevant for reward instead of the shapes. Once monkeys learned which dimension and stimulus was rewarded and reached criterion, the previously incorrect stimulus in the same dimension was now the rewarded stimulus and vice versa (ED shift reversal). Monkeys were tested in 60 min daily testing sessions. In that timeframe, there was no limit to how many trials, reversals, and stages they went through, although performance did not carry over between sessions for contribution to criterion. On subsequent testing days, the new session began on the stage last presented in the previous session. For each trial, monkeys had 30 s to make a stimulus choice, a 3 s intertrial interval, and a 5 s blank screen timeout following an incorrect response. Performance on each stage was assessed by the number of trials needed to move to the next stage, the number of correct/incorrect responses, and misses/omission errors. The number of misses, hits, and errors were also normalized to the number of trials each monkey underwent for each stage as this was variable based on performance.

Neuroimaging
MRI was performed at ~6, 12, 24, 36, and 45 months of age using a Siemens Magnetom Skyra 3-T with an 8-channel coil optimized for monkey brain scanning (RapidMR). Twenty-four of the animals were also scanned at 1 month of age. However, because of the low gray matter (GM)/white matter (WM) contrast in the T1 images, this time point is not included in the analyses for the current paper. Three animals were scanned at 3 months of age. However, some respiratory difficulties were encountered at this age, and scans were discontinued to not put the animals at risk. It was determined that 3 of the animals were sensitive to isoflurane; therefore, at subsequent time points, these animals were scanned using propofol as the anesthetic. The rate of infusion varied to maintain the animal at a steady state of anesthesia. All other animals at all time points were sedated with ketamine for tracheal intubation, then anesthetized with isoflurane for positioning in an MR-compatible stereotaxic apparatus. Once the animal was placed in and centered at the midline of the stereotaxic apparatus, the 8-channel receiver coil was attached to the stereotaxic apparatus using a custom connector. The center point of the 8-channel coil was positioned at AP + 10 on the stereotaxic apparatus. The Skyra table was "landmarked" at AP + 10 so that the center of the animal's brain was at the isocenter of the MRI magnet. Anesthesia was maintained with isoflurane at 1.3%-2.0%. Fluids were maintained with a saline infusion at a rate of 10 ml/kg/h for the duration of the MRI scan.

Acquisition parameters. T1-weighted images (480 sagittal slices) were acquired with TR = 2500 ms, TE = 3.65 ms, flip angle = 7°, FOV 256 × 256, voxel size during acquisition 0.6 × 0.6 × 0.6 mm. Acquired images were interpolated during image reconstruction to 512 × 512 voxels with a final resolution of 0.3 × 0.3 × 0.3 mm. The structural imaging protocol was followed with additional sequences that will not be described in this paper.

Image processing. All images were processed by operators unaware of group assignment. T1-weighted images were aligned into common space (Shi et al., 2016), bias field corrected, and brain masked using AutoSeg_3.3.2 (Wang et al., 2014). Brain masks were manually corrected if necessary. Following this preprocessing, T1-weighted images were segmented into GM, WM, and cerebrospinal fluid (CSF) using NeosegPipeline_v1.0.8 (Cherel et al., 2015) (Fig. 1). Probabilistic tissue maps from structural multi-atlas templates were applied to each subject's T1-weighted images via deformable registration. University of North Carolina lobar parcellation was used to parcellate the tissue segmentations into 24 lobar brain regions using the multi-atlas fusion in AutoSeg_3.3.2 (Wang et al., 2014). For these regions, total GM and WM volumes were extracted. Lateral ventricles volume were determined via semiautomated segmentation using the region competition deformable surface approach in ITK snap (Yushkevich et al., 2006) as applied to the probability CSF maps from the tissue segmentation (Lyall et al., 2012). All segmentation and parcellation results were visually quality controlled. No major issues were detected for any of the results.

ROIs. In order to limit the number of comparisons, the ROIs selected were based on a review of literature documenting brain alterations associated with MIA: prefrontal, frontal, cingulate, and temporal limbic (including amygdala and hippocampus) regions (Fig. 2), and lateral ventricles (Piontkewitz et al., 2011; Willette et al., 2011; Crum et al., 2017; Drazanova et al., 2018).

Statistical analysis
Statistical analyses were conducted within a generalized linear mixed-effects models framework (McCulloch et al., 2008) that can accommodate traditional GLMs (e.g., ANOVA and multiple linear regression) for data that

Table 6. Descriptive statistics (mean, SD) for temperature (°C) changes during poly ICLC (for MIA) or saline (for control) injections

	GD 43		GD 44		GD 46	
	MIA ($n = 14$) Mean (SD)	Control ($n = 10$) Mean (SD)	MIA ($n = 14$) Mean (SD)	Control ($n = 10$) Mean (SD)	MIA ($n = 14$) Mean (SD)	Control ($n = 10$) Mean (SD)
Time point for temperature reading						
Pre-infusion[a]	36.6 (0.7)	36.2 (1.6)	36.7 (0.8)	36.7 (0.7)	36.6 (0.6)	36.9 (0.6)
30 min	36.8 (0.9)	37.0 (0.7)	36.4 (0.9)	36.9 (0.6)	36.6 (0.6)	37.1 (0.6)
6 h	37.9 (0.6)	36.5 (0.7)	37.6 (0.8)	36.6 (0.5)	37.8 (0.8)	36.9 (0.7)
8 h	37.3 (0.6)	36.6 (0.8)	37.3 (1.0)	36.5 (0.7)	37.0 (1.2)	36.5 (1.1)

[a]Pre-infusion temperatures were recorded immediately before the injection (within 1-2 min).

were assumed normally distributed and independent across individuals, as well as linear mixed-effects models for normally distributed, binary, or count data that were collected repeatedly for an individual (across time or conditions). This flexible approach allows the use of all available data for an individual and provides the ability to control for the effect of covariates of interest and to account for the intrinsic complexity of the data by modeling subject-specific random effects and residual correlations. Transformations were used if assumptions of the linear models were not met and nonparametric techniques (exact Wilcoxon rank-sum test) were used to compare groups when transformations were unsuccessful. All models were validated both graphically and analytically. All tests were two-sided, with $\alpha = 0.05$. All analyses were conducted in SAS version 9.4. (SAS Institute).

Offspring development analyses. Developmental trajectories for weight, crown-rump, and head circumference were analyzed using linear mixed-effects models with fixed effects for group (MIA, control), age at measurement, and the interaction between age and group. Linear, quadratic, and cubic age effects were considered. To account for the within-animal dependence, random intercepts and slopes for linear and quadratic effect of age were included in the models.

Cognitive development analyses. Cognitive developmental outcomes were analyzed using repeated-measures techniques: linear mixed-effects models for continuous outcomes (after square root transforming the data to meet distributional assumptions) and logistic mixed-effects models (for events observed across trials, such as misses, correct choices, false alarms). To account for the within-animal dependence, random intercepts were included in the models. For the CPT, we modeled the number of misses and false alarms and the probability to commit a miss or a false alarm (using logistic models) across the trials in each session. Models included fixed effects for group (MIA, control), session (linear, quadratic, and cubic session effects), and the interaction between session and group. Interaction terms were not significant and were not retained in the reported models. For ID/ED shift, we modeled the miss and correct rates and the probability of a miss or correct choice (using logistic models) across the trials in each stage. Models included fixed effects for group (MIA, control), stage (categorical 8 stages), and their interaction. The interaction terms were removed if they were not significant. For RL tasks, nonparametric statistics were used to examine group differences in performance during individual sessions following the first reversal.

MRI analyses. The primary aim of the MRI analyses was to model brain growth from 6 to 45 months and to assess whether MIA-treated animals had a different developmental trajectory than the control animals. Separate models were fitted for each of the global measures (brain volume, GM, WM, lateral ventricles). We first fitted models with fixed effects for group (MIA, control), time (6, 12, 24, 36, or 45 months), and the interaction between group and time, using an exchangeable within-animal covariance (except for lateral ventricles, for which a spatial exponential covariance was used) to account for the correlated nature of the data because of the repeated measures. If the interaction did not add significantly to the model, it was removed, and the results of the model including only main effects were reported. For ROI analyses, two sets of models were fitted. The first set of models paralleled the global measures analyses; the second set included adjustment for the total brain volume. Separate models were fitted for GM and WM bilateral volumes in frontal, prefrontal, cingulate, and temporal limbic cortices. The core models
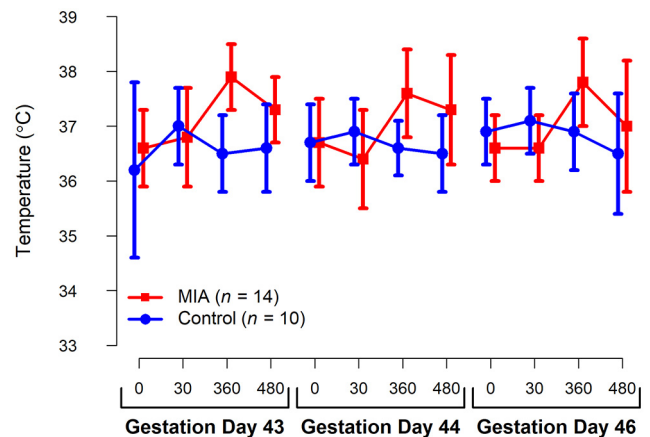
Figure 3. Average temperature for the MIA- and saline-treated dams from pre-infusion (0) through 480 min after infusion during GDs 43, 44, and 46. Vertical bars represent 1 SD.
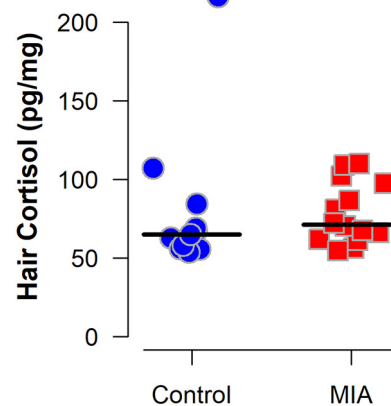
Figure 4. Hair cortisol concentration from MIA-exposed ($n = 14$) and Control ($n = 11$) dams. The Control group includes all 10 dams that received saline injections and one untreated dam enrolled before hair sample collection at GD 150. Horizontal lines indicate group medians. Wilcoxon rank-sum exact test indicated the groups did not differ ($p = 0.32$).

included fixed effects for group (MIA, control), time (6, 12, 24, 36, or 45 months), interaction between group and time, and total brain volume (for the adjusted models). Within-animal dependence was modeled using an unstructured covariance structure. We removed the interaction from the reported models if it was not significant. Significant interactions between group and time were followed up by tests to evaluate time-specific group differences.

Maternal cytokines and offspring neurodevelopment. A comprehensive evaluation of the maternal cytokine response and offspring development (i.e., behavior, multimodal neuroimaging, immune development) will be the focus of future publications. Here we present an exploratory evaluation of the relationship between maternal IL-6 and volumetric brain growth summaries of MIA-treated offspring. Spearman's rank

Table 7. Summary for the morphometric measures from 1 to 45 months

	Age (d) Mean (SD) [range]		Weight (kg) Mean (SD) [range]		Crown-rump (cm) Mean (SD) [range]		Head circumference (cm) Mean (SD) [range]	
	MIA (n = 14)	Control (n = 14)	MIA (n = 14)	Control (n = 14)	MIA (n = 14)	Control (n = 14)	MIA (n = 14)	Control (n = 14)
Evaluation time (mo)								
1[a]	31 (2) [28-35]	32 (7) [28-54]	0.7 (0.1) [0.5-0.8]	0.7 (0.2) [0.4-1.0]	22.4 (1.2) [20.5-24.5]	21.9 (1.3) [19.3-24.0]	20.8 (0.7) [19.5-21.8]	21.1 (0.8) [19.5-22.4]
3	91 (2) [88-94]	91 (1) [88-92]	1.0 (0.1) [0.8-1.3]	1.0 (0.3) [0.6-1.7]	25.1 (1.4) [22.7-28.0]	24.7 (1.9) [20.2-28.5]	22.2 (0.9) [20.9-23.9]	22.5 (1.0) [20.2-24.1]
6	180 (2) [177-182]	180 (1) [177-181]	1.5 (0.2) [1.3-1.8]	1.5 (0.2) [1.1-1.8]	30.1 (1.8) [27.0-33.0]	30.2 (2.1) [27.0-33.5]	23.4 (0.6) [22.5-24.5]	23.9 (1.2) [21.2-26.0]
12[b]	365 (2) [364-369]	365 (1) [364-366]	2.3 (0.3) [1.9-2.9]	2.3 (0.3) [1.8-2.9]	35.8 (1.4) [34.0-38.0]	35.2 (3.1) [30.0-39.0]	24.7 (0.6) [23.8-26.0]	24.9 (0.8) [23.5-26.5]
24[b]	730 (1) [729-733]	730 (1) [729-732]	3.7 (0.5) [2.9-4.6]	3.8 (0.6) [2.8-4.7]	41.9 (2.0) [38.1-45.0]	41.9 (1.9) [38.3-44.7]	26.5 (1.0) [24.5-28.6]	27.2 (1.3) [24.5-29.5]
36[b]	1095 (1) [1093-1096]	1099 (8) [1092-1116]	5.6 (0.9) [4.5-6.9]	5.6 (1.0) [4.2-7.3]	48.6 (1.9) [45.5-51.0]	48.0 (2.9) [43.7-52.0]	28.5 (1.2) [26.4-30.2]	29.0 (1.2) [27.0-31.5]
45[c]	1372 (2) [1368-1374]	1371 (2) [1368-1374]	7.5 (1.0) [6.1-8.8]	7.4 (1.1) [5.6-8.9]	52.4 (1.7) [50.0-55.2]	52.1 (2.9) [47.0-57.0]	30.7 (1.3) [28.2-32.6]	30.6 (1.1) [28.4-32.1]

[a]Data missing for 1 MIA and 2 Control animals for crown-rump and 1 MIA and 1 Control for head circumference.
[b]Data missing for 1 MIA animal on all variables because of death.
[c]Data missing for 2 MIA animals on all variables because of death.
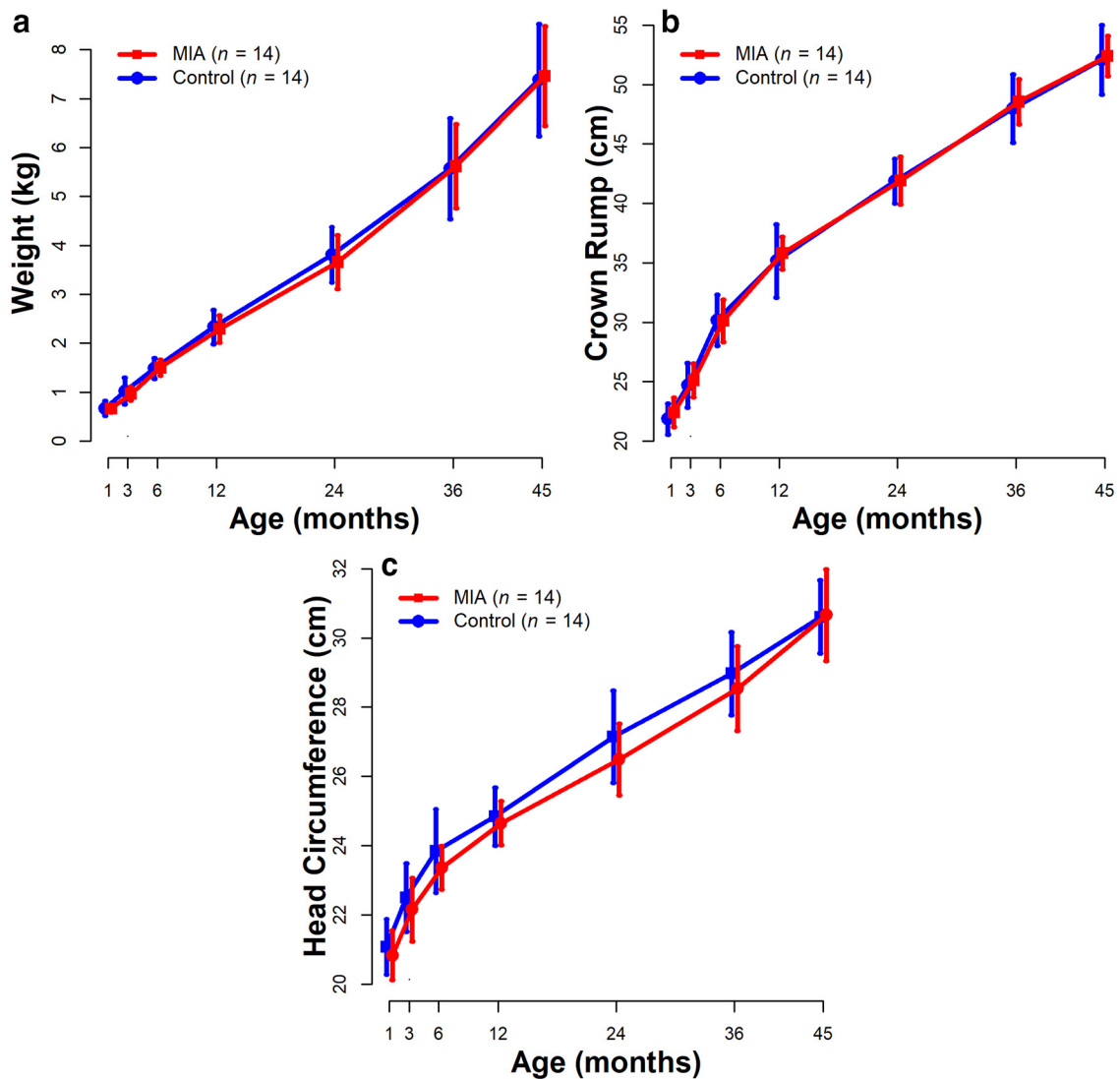
Figure 5. Average trajectory for weight (**a**), crown-rump length (**b**), and head circumference (**c**) for the MIA-exposed and Control offspring from 1 month through 45 months. Vertical bars represent 1 SD.

correlations examined the associations between maternal IL-6 response and frontal and prefrontal GM and WM brain volumes in the offspring after reducing the serial data for each individual to summaries reflecting relevant and interpretable aspects of the data. Maternal IL-6 response was summarized by the peak level (i.e., the maximum) after second and third injections, which may be interpreted as a maximum effect of the injection. Because the imaging was performed at unequal time intervals and there was small variation in the ages at scan across offspring, each monkey's GM ROI trajectory was summarized by calculating the area under the curve, standardized by the length in the study. These

Table 8. Summary of week 1 neuro-motor reflexes, behavioral maturation, and attention[a]

	MIA (n = 14)		Control (n = 14)		
	Mean (SD)	Median [range]	Mean (SD)	Median [range]	p[b]
Age (d)	7.0 (0.7)	7.0 [6.0-8.0]	6.9 (0.6)	7.0 [6.0-8.0]	0.95
Weight (kg)[c]	0.5 (0.1)	0.5 [0.5-0.7]	0.6 (0.1)	0.6 [0.4-0.7]	0.49
Gestation length (d)	168 (4)	167 [162-175]	167 (4)	167 [160-177]	0.97
Visual orientation	1.3 (0.6)	1.3 [0-2]	1.7 (0.4)	1.8 [1-2]	0.14
Visual follow	0.9 (0.4)	1.0 [0.5-1.5]	1.1 (0.6)	1.0 [0-2]	0.23
Head posture	2.0 (0.0)	2.0 [2-2]	2.0 (0.0)	2.0 [2-2]	1.00
Coordination	0.8 (0.8)	0.8 [0-2]	0.7 (0.7)	0.8 [0-2]	0.96
Spontaneous crawl	1.1 (0.7)	1.0 [0-2]	0.9 (0.7)	1.0 [0-2]	0.38
Rooting	0.6 (0.9)	0.0 [0-2]	0.4 (0.7)	0.0 [0-2]	0.78
Righting	1.9 (0.5)	2.0 [0-2]	1.9 (0.5)	2.0 [0-2]	1.00
Placing	1.1 (0.8)	1.0 [0-2]	0.8 (0.8)	0.8 [0-2]	0.36
Moro reflex[d]	1.8 (0.3)	2.0 [1-2]	1.7 (0.4)	2.0 [1-2]	0.76
Predominant state	0.9 (0.5)	1.0 [0-2]	0.6 (0.6)	0.5 [0-2]	0.19
Consolability	0.5 (0.7)	0.0 [0-2]	0.3 (0.6)	0.0 [0-1.5]	0.36

[a]All animals were rated with a score from 0 to 2 (0 = reflex absent; 0.5 = reflex slightly developed or present; 1 = partially present or partially developed; 1.5 = mostly present or developed; 2 = reflex present or fully developed). Predominant state: 0 = calm, alert, aware; 0.5 = mostly calm with slight agitation; 1 = alert but agitated for no more than half the examination; 1.5 = agitated for more than half the examination; 2 = extremely agitated throughout entire examination. Consolability: 0 = quickly consoled when picked up following examination; 0.5 = consoled after brief period of holding and swaddling; 1 = infant consoled only after prolonged holding, swaddling, rocking, and/or stroking; 1.5 = brief moments of consolation and quiet after prolonged holding; 2 = inconsolable.
[b]From Wilcoxon two-sample exact tests.
[c]Data missing for 2 animals in MIA group.
[d]Data missing for 1 animal in MIA group.

Table 9. Summary of pre-wean (weeks 9-24) home cage observations[a]

	MIA (n = 14)		Control (n = 14)		
	Mean (SD)	Median [range]	Mean (SD)	Median [range]	p
Breast contact	2.4 (0.8)	2.6 [1.2-3.6]	2.7 (0.8)	2.7 [1.5-3.9]	0.36
Other contact	0.7 (0.3)	0.6 [0.2-1.2]	0.8 (0.5)	0.7 [0.2-2.1]	0.96
Ventral contact	1.5 (0.9)	1.3 [0.4-3.8]	1.5 (0.6)	1.4 [0.5-2.6]	0.98
No contact	3.4 (0.9)	3.4 [1.8-4.8]	3.2 (0.8)	3.1 [2.0-4.4]	0.48
Maternal restrain	0.02 (0.04)	0.1 [0-0.13]	0.01 (0.02)	0 [0-0.07]	0.08
Maternal retrieve	0.04 (0.05)	0.02 [0-0.19]	0.03 (0.03)	0.03 [0-0.10]	0.88
Maternal reject	0.11 (0.12)	0.07 [0-0.44]	0.08 (0.08)	0.06 [0-0.31]	0.68
Total explore[b]	0.4 (0.2)	0.4 [0.1-0.7]	0.4 (0.1)	0.4 [0.2-0.6]	1.00
Total stereotypies[c]	0.003 (0.01)	0 [0-0.3]	0.004 (0.1)	0.0 [0-0.2]	0.52

[a]Infants were observed up to 5 times per week between 2 and 6 months. For each animal and each week, behaviors were first averaged over the observations that were available (ranging from 3 to 5). All animals had data between 9 and 24 weeks, so we then averaged the behaviors again within animals (from 9 to 24 weeks), to create a summary over the course of the study. Wilcoxon rank-sum exact tests were then fitted to these averaged behaviors.
[b]Total explore includes toy play, oral explore, and manual explore.
[c]Total stereotypy includes pace, head twist, backflip, bounce, nipple clasp, rock, swing, self-bite, and salute.

correlations were conducted separately in the two groups, using only the monkeys who had complete data (12 MIA, 10 Control).

Results

Validation of MIA
Blood samples collected 6 h after the second (GD 44) and third (GD 46) Poly ICLC injections confirmed a strong proinflammatory cytokine response as indexed by change in IL-6 from baseline samples (Table 4). Within the control group, the highest measurable IL-6 value (peak) was significantly positively correlated with dam age at conception (Spearman's rank correlation = 0.80, $p = 0.005$), but not significantly correlated with weight ($p = 0.11$). Within the MIA group, there was no significant correlation between peak IL-6 levels and maternal age ($p = 0.31$) and weight ($p = 0.85$). Dams that received Poly ICLC injections also

Table 10. Summary of post-wean (weeks 34-78) home cage observations[a]

	MIA (n = 14)		Control (n = 14)		MIA vs control estimated difference (SE)	p[b]
	Mean (SD)	Median [range]	Mean (SD)	Median [range]		
Sleep[c]	0.03 (0.05)	0 [0-0.1]	0.04 (0.03)	0.04 [0-0.1]	−0.07 (0.05)	0.20
Nonsocial[c]	3.3 (0.6)	3.5 [2.2-4.3]	3.4 (0.6)	3.4 [2.0-4.1]	0.04 (0.04)	0.30
Proximity	4.0 (0.5)	4.0 [3.3-4.7]	3.9 (0.5)	3.8 [3.1-4.8]	0.07 (0.17)	0.68
Contact[c]	0.5 (0.2)	0.5 [0.1-0.8]	0.5 (0.2)	0.5 [0.1-1.1]	0.01 (0.06)	0.92
Play[c]	1.0 (0.3)	0.9 [0.5-1.4]	0.9 (0.3)	0.8 [0.5-1.4]	−0.05 (0.04)	0.31
Composite activity[c]	0.5 (0.3)	0.4 [0.2-1.1]	0.6 (0.3)	0.5 [0.2-1.1]	−0.04 (0.08)	0.67
Composite stereotypies[c]	0.2 (0.3)	0.1 [0-0.8]	0.2 (0.3)	0.1 [0-1.0]	0.02 (0.12)	0.87

[a]Infants were observed 3 times per week between 27 and 85 weeks. For each animal and each week, behaviors were first averaged over the three observations that were available. Not all animals were observed each week; all animals had data between 34 and 78 weeks, so we then averaged each type of behavior again within animals (from 34 to 78 weeks), to create summary behaviors over the course of the study. To these summary behaviors, we fitted linear mixed-effects models with a fixed effect for group and a random effect for the "play buddy" to account for the fact that animals interacted in pairs and the exhibited behaviors were correlated (Standard error, SE.).
[b]From linear mixed-effects models.
[c]Data were square root transformed for the analysis.

exhibited transient sickness behaviors, including reduced appetite and fever (Tables 5 and 6; Fig. 3). There was no significant difference in hair cortisol concentration between groups collected at the end of the third trimester (GD 150) (Fig. 4). Notably, the hair cortisol concentrations observed in the MIA-treated dams during late gestation were similar to those observed in other multiparous and laboratory-housed pregnant rhesus macaques that were not undergoing any further experimental manipulations (Dettmer et al., 2015), suggesting that the protocol used for inducing and assessing MIA was not associated with lasting changes in stress as indexed by hair cortisol.

Offspring development
There were no group differences in overall health, physical development (Table 7; Fig. 5) and neuromotor reflexes, behavioral maturation, and attention (Table 8). There were also no significant group differences detected in the home cage observations with their mothers from 9 to 24 weeks of age (Table 9) or when observed interacting with a treatment-matched social partner in the home cage from 34 to 78 weeks of age (Table 10).

Cognitive development
RL
Overall performance was similar between groups as all monkeys achieved at least one reversal; however, the number of monkeys meeting criterion on subsequent reversals diminished steadily in a non–group-specific manner. Only the sessions up to and including the first reversal were analyzed as this was the only reversal all subjects achieved. There was no significant difference in the percent errors made between the two groups either before or after the first reversal as demonstrated in Figure 6a. However, following the first reversal, MIA-treated offspring had a significantly higher number of omission errors (Fig. 6b), a trial in which they failed to give a response within the 30 s timeframe. Temperament scores following the first reversal session rated behavior of the majority of the MIA-treated animals during omission error trials as "apathetic/inactive" (data not shown). Temperament scores for object orientation, goal directivity, irritability, activity, inhibition, impulsivity, stereotypies, and attention did not differ between groups.

CPT

Groups performed similarly on most CPT measures, such as hit rate, number of misses (omission errors), average correct rejections, response bias (β), signal detection theory measures of response accuracy (d'), and nonresponse bias (c) (Fig. 7a–f). However, the MIA-treated group was significantly more likely to false alarm (Fig. 7g) in a mixed-effects logistic model (odds ratio = 1.81, $p = 0.03$). The group difference in square root transformed number of false alarms did not reach statistical significance ($p = 0.08$).

PRBT and PRL

Performance on the PRBT was similar between groups with no differences observed on the highest ratio completed, session length, total number of responses, or total reinforcers earned between the two groups (Fig. 8a–d). The groups also had similar performance on

Figure 6. Performance on RL task of MIA-exposed (n = 13) and Control (n = 14) offspring at 21 months of age. Scatterplots show the following: (a) mean error percent during the initial acquisition stage and the reversal stage and (b) number of omission errors (i.e., nonresponses) in the session following the first reversal. Horizontal lines indicate group medians. ∗∗Compared with the Control group, MIA offspring have more omission errors (p = 0.005 using Wilcoxon exact rank-sum test).
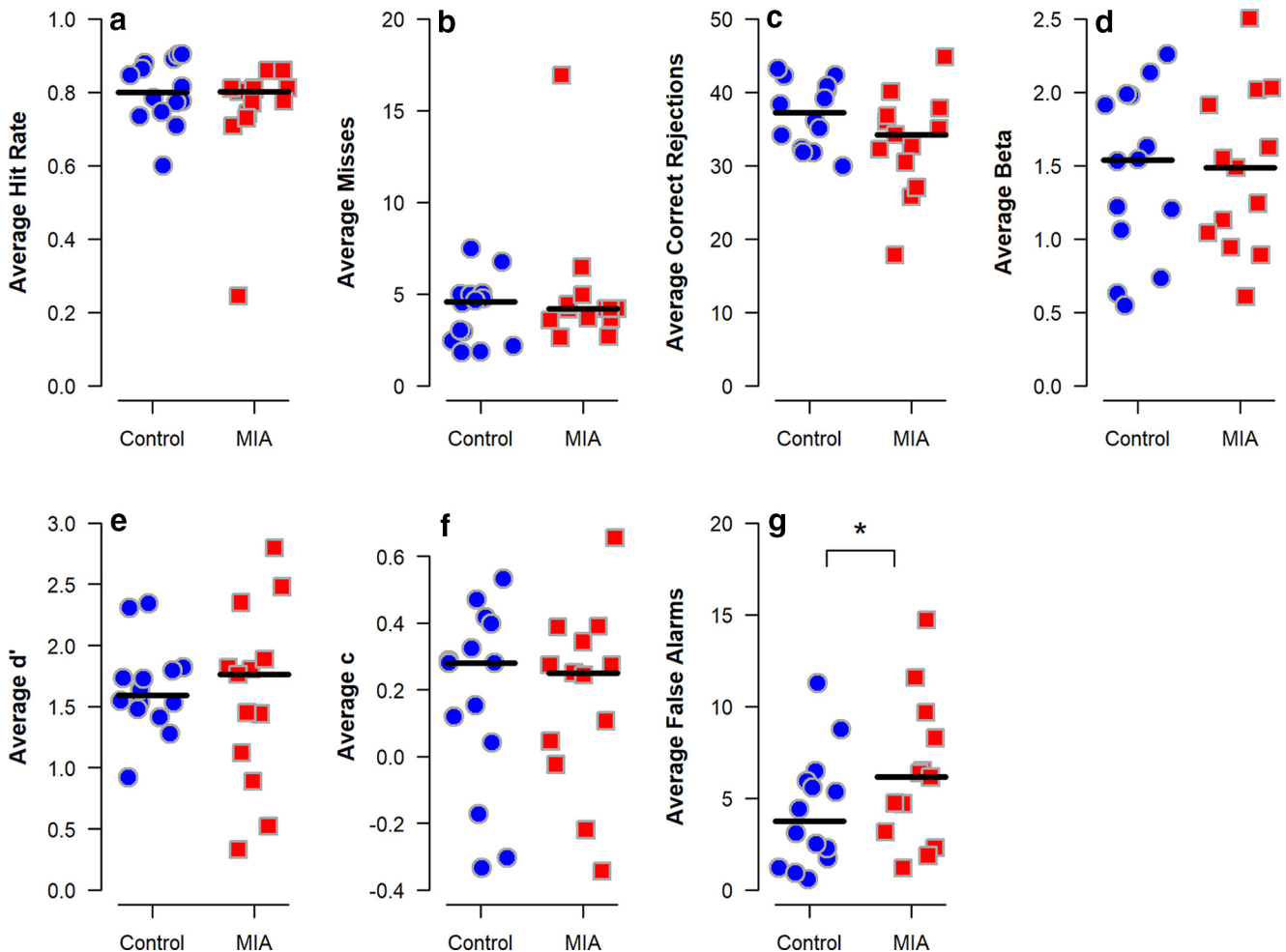
Figure 7. CPT performance of MIA-exposed (n = 13) and Control (n = 14) offspring at 33–34 months of age. Scatterplots show performance endpoints averaged across 20 testing sessions as follows: (a) hit rate (correct responses), (b) misses (omission errors), (c) correct rejections (not selecting an incorrect box), (d) β (response bias), (e) d' (response accuracy), (f) c (nonresponse bias), and (g) false alarms (selecting an incorrect box). Horizontal lines indicate group medians. ∗Compared with the Control group, MIA offspring are more likely to commit false alarms (p < 0.05 using a mixed-effects logistic model).

Figure 8. PBRT performance of MIA-exposed ($n = 12$) and Control ($n = 14$) offspring at 40-41 months of age. The number of screen presses required to obtain a food reward (the "ratio") increased geometrically over the course of the 30 min session or until the monkey stopped responding for 3 min. Scatterplots show the following: (**a**) highest completed ratio, (**b**) duration of the test, (**c**) total number of responses, and (**d**) total reinforcers earned, averaged across the sessions for each individual. Horizontal lines indicate group medians. The groups did not differ.

the PRL task with each group having a similar number of sessions to reach the first reversal (Fig. 9a), performance after the first reversal (Fig. 9b), proportion of animals completing each reversal (Fig. 9d), and number of sessions to each reversal (Fig. 9e). Interestingly, there was no difference in the number of omission errors following reversals in this task (Fig. 9c). Similarly, win-stay lose-shift behavior did not differ between groups (data not shown).

ID/ED shift
Similar to past studies, both groups made significantly more errors during the ED shift than the ID shift, showing an attentional set had been formed (Baxter and Gaffan, 2007; Weed et al., 2008). No difference between groups was demonstrated by the number incorrect at each stage (Fig. 10a), the number of choice trials (Fig. 10c), or the error rate at each stage (Fig. 10d). However, during the SDR and CDR stages, the MIA-treated offspring was significantly more likely to miss (i.e., commit an omission error) in mixed-effects logistic models (SDR: odds ratio = 5.48, $p = 0.01$; CDR: odds ratio = 6.89, $p = 0.003$) (Fig. 10b). The group difference in square root transformed miss rate remained significant in linear mixed-effects model for SDR ($p = 0.01$) and approaches statistical significance for CDR ($p = 0.051$). No significant group differences in miss rate were observed for other stages.

Neuroimaging
Table 11 summarizes the volumetric measures for the two groups, and Table 12 displays the results of the linear mixed-

effects linear models for global measures. The two groups had parallel growth trajectories from 6 to 45 months on all global measures: that is, total brain volume, total gray and total WM volume, and lateral ventricle volume; none of the group × time interactions reached statistical significance. Total brain volume from 6 to 45 months for the MIA-treated animals was consistently smaller than for the control animals, although the difference was not significant (estimated difference [est.] = −5654 mm^3, $p = 0.12$). The same pattern of smaller volume in the MIA-treated animals relative to controls was present in total GM (est. = −3762 mm^3, $p = 0.12$).

Table 13 summarizes the results of the unadjusted analyses for GM and WM volumes in the four ROIs. For GM, the two groups had parallel developmental trajectories from 6 to 45 months in all four regions; none of the group × time interactions reached significance. Yet, for the GM in the frontal and prefrontal regions (Fig. 11a,b), MIA-treated monkeys had smaller volumes than controls did at 6 months, and these differences persisted at later ages. (frontal: est. = −564.6 mm^3, $p = 0.005$, prefrontal: est. = −695.8 mm^3, $p = 0.04$). Table 14 summarizes the results of the analyses after adjusting for total brain volume. The magnitude of the group differences decreased, but remained significant, in both frontal and prefrontal GM (frontal: est. = −403.3 mm^3, $p = 0.01$, prefrontal: est. = −387.6 mm^3, $p = 0.02$).

For frontal WM, there was an interaction between time and group in both unadjusted and adjusted analyses. The two groups had similar levels of frontal WM at 6 months, but had significantly different growth trajectories over time (Fig. 11c), resulting in the MIA group having lower volumes by 36 months (est. = −353.7 mm^3, $p = 0.047$) and more pronounced differences at 45 months (est. = −436.3 mm^3, $p = 0.02$). These differences persisted after adjusting for total brain volume, although the magnitude of the group differences decreased (36 months: est. = −187.0 mm^3, $p = 0.050$, 45 months: est. = −264.1 mm^3, $p = 0.01$). Furthermore, the growth of frontal WM volume from 6 months to 24, 36, and 45 months was significantly smaller in the MIA group relative to the Control group (Table 13). A similar effect was seen when adjusting for total brain volume, with frontal WM volume growth significantly smaller from 6 months to 12, 36, and 45 months in the MIA group relative to the Control group (Table 14).

Maternal cytokines and offspring neurodevelopment
The correlation analysis for MIA-treated animals revealed a consistent pattern of negative association between peak maternal IL-6 response and summary measures of both GM (Spearman's $\rho = −0.50$, $p = 0.10$ in prefrontal; $\rho = −0.55$, $p = 0.06$ in frontal) and WM ($\rho = −0.63$, $p = 0.03$ in prefrontal; $\rho = −0.62$, $p = 0.03$ in frontal) in prefrontal and frontal regions. No pattern of association was detected in the Control group (correlations between −0.07 and 0.02, all $p > 0.85$).

Discussion
Here we present initial results from a new cohort of male MIA-treated NHP offspring undergoing a comprehensive assessment of brain and behavioral development from birth through 4 years of age, a time frame spanning early infancy through late adolescence. We have previously demonstrated that rhesus monkeys exposed to prenatal immune challenge develop aberrant behaviors after a period of early typical development (Bauman et al., 2014; Machado et al., 2015; Careaga et al., 2017). Although
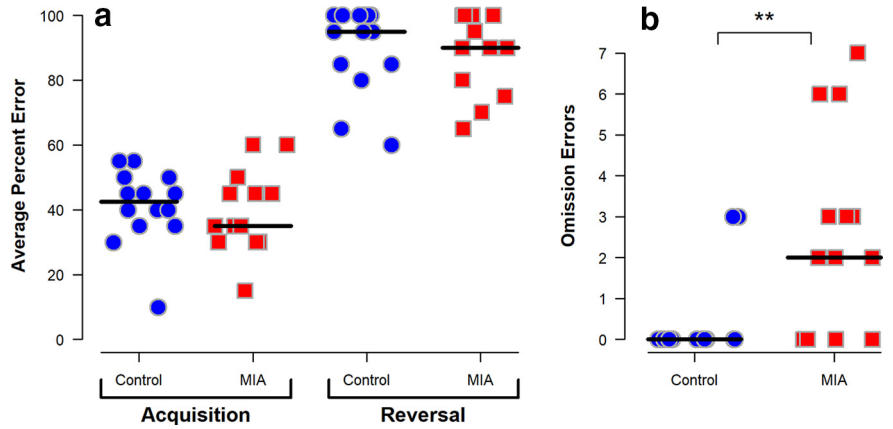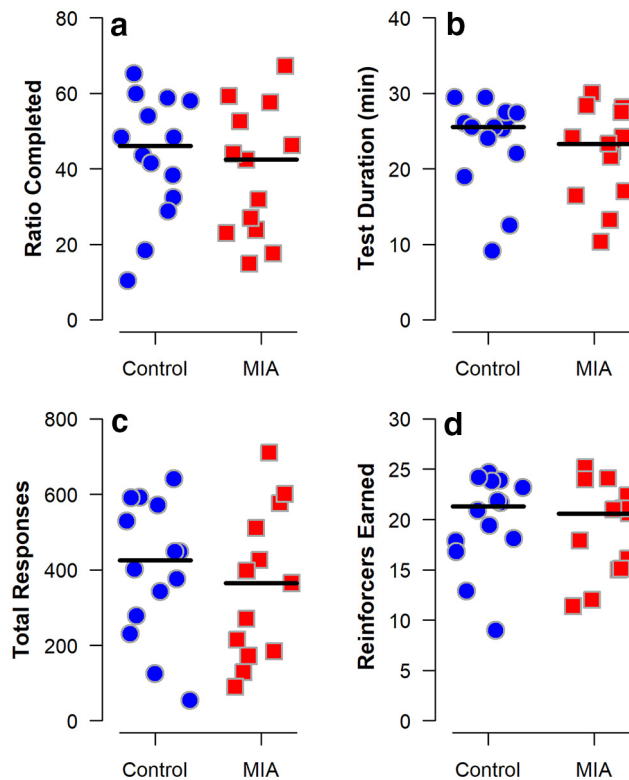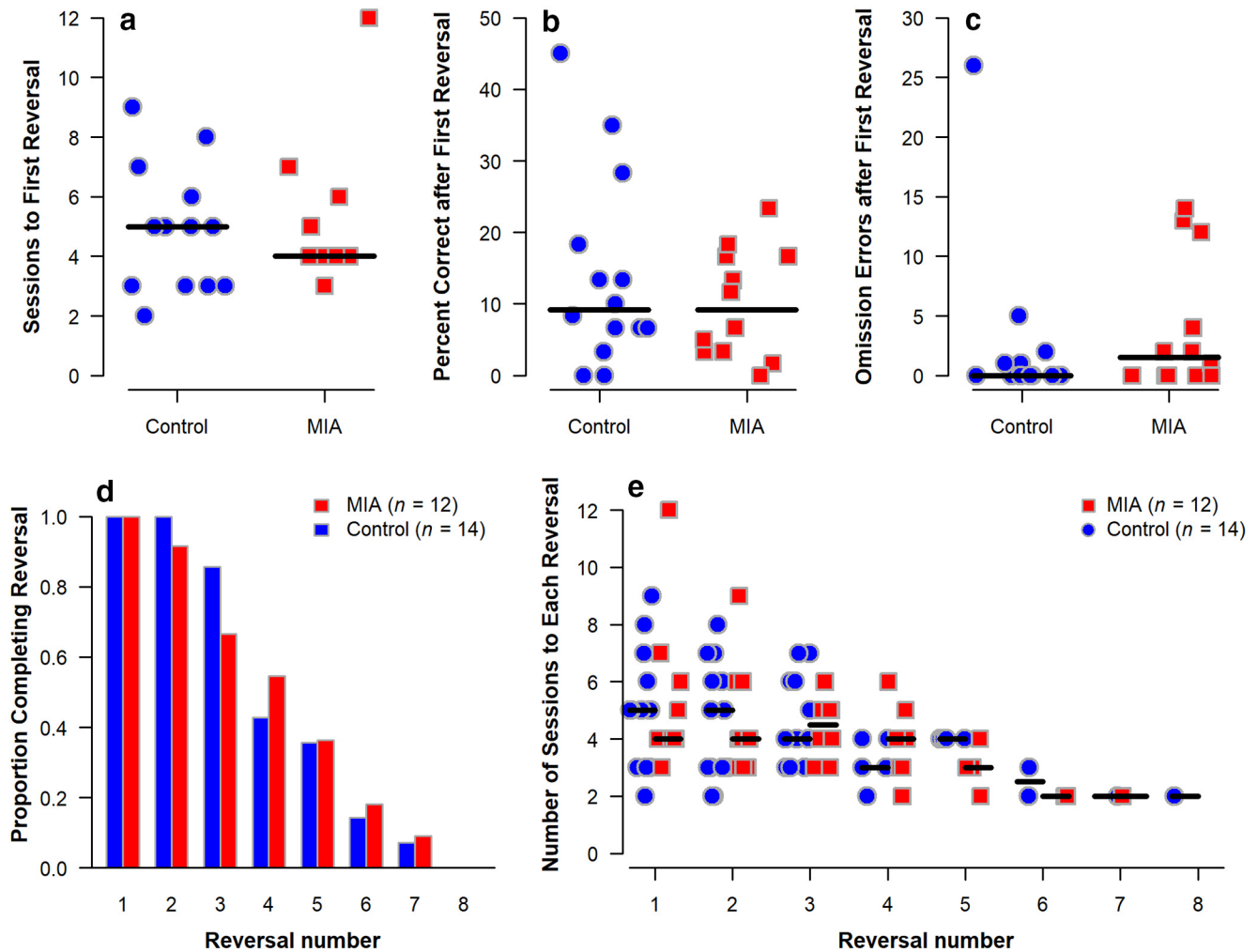
Figure 9. PRL task performance of MIA-exposed ($n = 12$) and Control ($n = 14$) offspring at 44-45 months of age. Plots show the following: (**a**) number of sessions required to meet criteria for the first reversal, (**b**) percent correct in the session following the first reversal, (**c**) number of omission errors following the first reversal, (**d**) proportion of animals in each group achieving each reversal, and (**e**) number of sessions required to meet criteria for each reversal. Horizontal lines indicate group medians. The groups did not differ.

evidence of increased striatal dopamine was detected in late adolescence (Bauman et al., 2019), other aspects of neurodevelopment have not been explored in the NHP MIA model. Here we describe striking reductions in frontal lobe volume throughout development paired with the emergence of subtle changes in cognitive performance detected in the first evaluation of cognitive development in a NHP MIA model. These findings demonstrate the translational utility of the NHP model to evaluate the emergence of neurodevelopmental changes in a species more closely related to humans and to highlight ongoing developmental changes in the anatomy of the frontal lobes as a potential marker of MIA-induced risk.

Compared with controls, the MIA-treated offspring exhibited reductions in frontal and prefrontal GM volumes at 6, 12, 24, 36, or 45 months and smaller increases in frontal WM, resulting in significantly reduced WM volumes at the latter time points. Volumetric reductions have emerged as a consistent outcome in rodent MIA models (for review, see Guma et al., 2019) and have also been reported following prenatal influenza exposure in NHPs (Short et al., 2010). Although comparing developmental trajectories across species is challenging, it is noteworthy that reduced frontal volume has been detected in both mid-gestation MIA-treated rats (Piontkewitz et al., 2012; Crum et al., 2017) and

late first trimester MIA-treated NHPs. Delay in frontal WM growth volume emerging in MIA-treated offspring between 2 and 3 years of age observed in this study indicates a deviation from the species-typical increased WM volumes seen from birth through puberty (Malkova et al., 2006; Knickmeyer et al., 2010). These findings highlight the frontal lobe as a particularly vulnerable region to prenatal immune challenge in NHPs, which is consistent with our preliminary findings of subtle changes in DLPFC dendritic morphology (Weir et al., 2015). Indeed, rodent MIA models have also identified numerous changes in neuronal migration, number, density, and alterations in dendritic structure and synapse formation that could contribute to aberrant brain growth trajectories (for review, see Bergdolt and Dunaevsky, 2019). In the present study, dams received Poly ICLC injections on GD 43, 44, and 46, which corresponds to late first trimester (GD 0-55) of the 165 d gestation. In rhesus monkeys, first trimester peak neurogenesis of subcortical structures is followed by the early stages of corticogenesis that continues through the second trimester (GD 56-110) (Rakic, 1988). Emerging evidence indicates that microglia play a critical role in regulating cell production during this time and raises the possibility that MIA-induced changes in the maternal-fetal immune
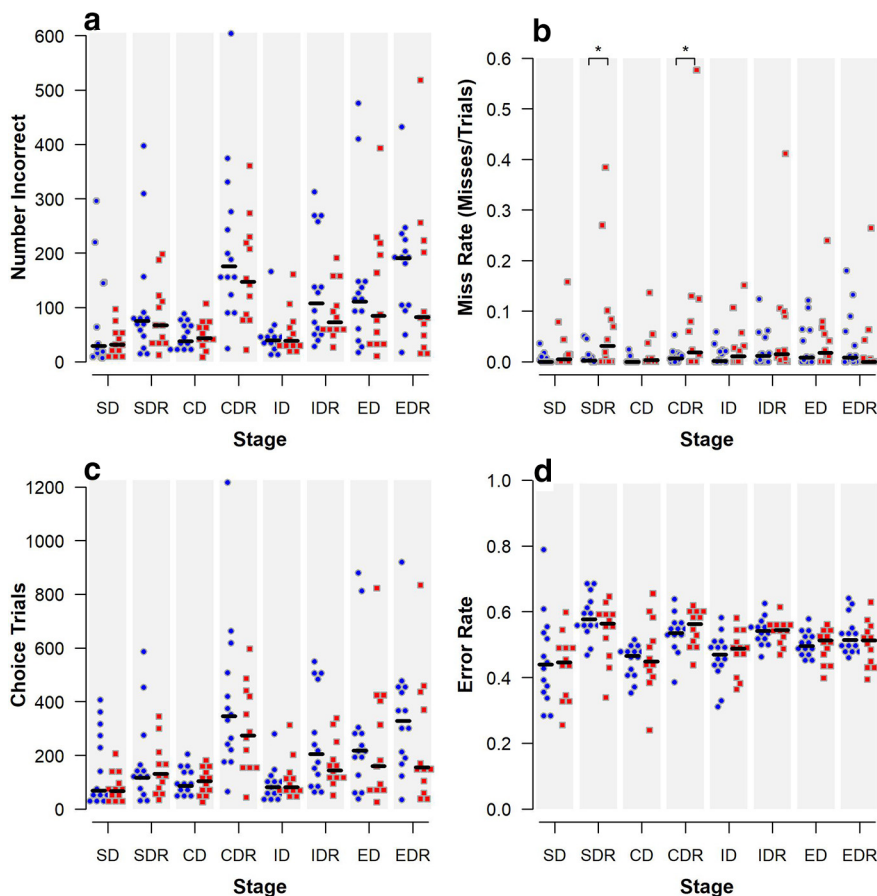
Figure 10. Performance on ID/ED shift initiated at 46-47 months of age of MIA-exposed (*n* = 12) and Control (*n* = 14) offspring. Scatterplots show the following: (*a*) number of incorrect responses, (*b*) miss rate, (*c*) number of choice trials, and (*d*) error rate for each stage. Horizontal lines indicate group medians. *Compared with the Control group, MIA offspring are more likely to miss during SDR and CDR ($p < 0.05$ using mixed-effects logistic models). SD, Simple discrimination; SDR, Simple discrimination reversal; CD, compound discrimination; CDR, Compound discrimination reversal; ID, Intradimensional shift; IDR, ID shift reversal; ED, Extradimensional shift; EDR, ED shift reversal.

environment could alter the timing and trajectory of these critical neurodevelopmental processes (Barger et al., 2019).

Despite the significant reduction in GM and WM volumes observed in the MIA-treated animals as described above, the MIA-treated animals had similar overall cognitive performance to control groups with some subtle differences. The MIA-treated offspring showed evidence for increased omission errors in the RL and more misses during two stages of the ID/ED (both reversal stages), which are measures of the subject not providing a response. These behavioral changes may reflect difficulty adaptively forming and using a task set but could also reflect an increased impact of unexpected negative feedback on MIA performance. Given that MIA-treated animals performed similarly to controls on all endpoints of PRBT, motivation does not appear to be a major contributing factor. Additionally, the MIA offspring also had a significantly increased number of false alarms on the CPT. When tested with a PRL paradigm at 4 years of age, no differences were found in overall performance or number of omission errors observed. The different outcomes in omission errors in the RL task versus the PRL could be a factor of maturity or a result of the different testing parameters. In the PRL task, the monkey would have an expected slowed rate of learning requiring a more complex strategy to achieve a reward compared with the RL task, and the increased complexity could have

resulted in improved task engagement (Izquierdo and Jentsch, 2012). In both the RL and ID/ED task, when the MIA offspring were engaged and participating, their performance was similar to the control group.

Overall, it appears the MIA offspring performed similarly to controls but had occasional trouble maintaining and using the rule associated with the tasks. It is important to note that the NHPs in the current study were evaluated from infancy through late adolescence, when cognitive performance strategies continue to mature (Weed et al., 1999). It is plausible that the subtle changes in early cognitive performance observed in these young MIA-treated monkeys may represent a "prodromal" phase in the model that may become more pronounced over time as the monkeys progress from adolescence to young adulthood. Indeed, although many studies using an adult rodent MIA model have described impairments in working and spatial memory (Bergdolt and Dunaevsky, 2019; Haddad et al., 2020), studies testing juvenile age groups have produced mixed results with some reporting various deficits in cognition during prepubescent time points (Vuillermot et al., 2012; Giovanoli et al., 2015), whereas others found deficits that only emerged during adulthood (Meyer et al., 2006; Richetto et al., 2014).

Our NHP Poly IC-based MIA model is designed to stimulate inflammatory cytokine response late in the first trimester that mimics a moderate to severe infection during pregnancy. The MIA-treated dams exhibit transient fever, reduced appetite, and elevated inflammatory cytokines, including IL-6, which is necessary and sufficient for MIA to alter brain development and behavior in rodent offspring (Smith et al., 2007) and has recently been associated with neurodevelopmental outcomes in monkeys (Ramirez et al., 2020) and humans (Rasmussen et al., 2021). Although the MIA model has historically been presented as a model relevant for ASD and/or SZ, emerging consensus in the field suggests that prenatal immune challenge may serve as a "disease primer" that, in combination with other genetic or environmental factors, may result in altered brain and behavior trajectories relevant to a number of NDDs (Meyer, 2019). While comparisons between animal models and clinical disorders must be made with caution, the NHP model more closely approximates the protracted period of postnatal development needed to evaluate the emergence of MIA-induced neurodevelopmental changes. The subtle impairments of cognitive performance exhibited by the MIA-treated animals does align with the premorbid phase of SZ, characterized by attentional and other cognitive deficits in later childhood and adolescence (McCutcheon et al., 2020) that become more severe over time (Guo et al., 2019). The reductions in cortical GM volume observed in this new cohort of MIA-treated monkeys also align with neuroimaging studies from adolescents and

Table 11. Summary for the GM and WM volumetric measures (mm³) from 6 to 45 months

	6 months		12 months		24 months		36 months		45 months	
	MIA (n = 14)	Control (n = 14)	MIA (n = 13)	Control (n = 14)	MIA (n = 13)	Control (n = 14)	MIA (n = 13)	Control (n = 14)	MIA (n = 12)	Control (n = 14)
Age (d) at scan, Mean (SD) [range]										
	180 (2)	181 (5)	365 (2)	365 (1)	730 (1)	730 (1)	1095 (1)	1099 (8)	1372 (2)	1371 (2)
	[177-182]	[177-199]	[364-369]	[364-366]	[729-733]	[729-732]	[1093-1096]	[1092-1116]	[1368-1374]	[1368-1374]
Global measures, Mean (SD)										
Total brain volume	81,429 (8113)	86,200 (7724)	83,522 (9692)	88,781 (8550)	87,821 (10,381)	94,268 (9060)	89,446 (9242)	95,287 (9372)	92,406 (10,297)	97,857 (9671)
GM	59,665 (6002)	63,271 (5146)	59,404 (6884)	63,073 (5538)	60,710 (7240)	65,058 (5710)	59,876 (5918)	63,474 (5735)	60,803 (6872)	64,164 (5941)
WM	21,764 (2245)	22,929 (2666)	24,118 (2889)	25,708 (3133)	27,111 (3270)	29,210 (3598)	29,570 (3480)	31,813 (3870)	31,604 (3579)	33,693 (4004)
Lateral ventricles	516 (186)	520 (180)	537 (248)	509 (190)	586 (344)	597 (185)	717 (367)	647 (184)	741 (407)	712 (192)
Frontal measures, Mean (SD)										
GM	6739 (651)	7433 (521)	6853 (812)	7594 (661)	7145 (910)	8068 (736)	7220 (790)	7971 (747)	7450 (985)	8039 (800)
WM	2594 (294)	2775 (330)	2899 (347)	3152 (377)	3359 (389)	3682 (411)	3681 (428)	4035 (448)	3919 (422)	4315 (480)
Prefrontal measures, Mean (SD)										
GM	6325 (853)	7128 (657)	6277 (949)	7078 (759)	6298 (991)	7169 (787)	6175 (819)	6942 (867)	6193 (946)	6961 (790)
WM	1586 (269)	1701 (242)	1830 (325)	2017 (284)	2151 (378)	2407 (340)	2338 (398)	2603 (364)	2479 (422)	2746 (391)
Cingulate measures, Mean (SD)										
GM	2156 (257)	2315 (239)	2136 (271)	2337 (249)	2137 (301)	2332 (261)	2092 (247)	2269 (237)	2089 (292)	2289 (251)
WM	334 (48)	370 (59)	362 (55)	405 (66)	417 (65)	472 (79)	453 (65)	511 (81)	480 (72)	535 (82)
Temporal limbic measures, Mean (SD)										
GM	2416 (189)	2441 (215)	2632 (241)	2738 (241)	2928 (319)	3017 (270)	2942 (308)	3034 (316)	2989 (336)	3077 (282)
WM	432 (48)	442 (49)	463 (52)	482 (56)	533 (65)	563 (68)	564 (61)	593 (83)	596 (60)	622 (74)

Table 12. Parameter estimates from the linear mixed-effects models for global volumetric measures[a]

	Total brain		GM		WM		Lateral ventricles	
Model term	Estimate (SE)	p	Estimate (SE)	p	Estimate (SE)	p	Estimate (SE)	p
Intercept	86,608 (2455)	<0.001	63,364 (1623)	<0.001	23,243 (882)	<0.001	523 (44)	<0.001
Difference (mm³) MIA vs Control	−5654 (3521)	0.12	−3762 (2322)	0.12	−1892 (1260)	0.15	−50 (59)	0.40
Difference (mm³) Time 2 vs Time 1	2363 (388)	<0.001	−247 (306)	0.42	2610 (181)	<0.001	−8 (18)	0.66
Difference (mm³) Time 3 vs Time 1	7278 (388)	<0.001	1411 (306)	<0.001	5867 (181)	<0.001	50 (28)	0.08
Difference (mm³) Time 4 vs Time 1	8589 (388)	<0.001	188 (306)	0.54	8401 (181)	<0.001	139 (34)	<0.001
Difference (mm³) Time 5 vs Time 1	11,123 (393)	<0.001	866 (310)	0.006	10,258 (184)	<0.001	187 (38)	<0.001

[a]Time 1 = 6 months; Time 2 = 12 months; Time 3 = 24 months; Time 4 = 36 months; Time 5 = 45 months. Mixed-effects linear regression models were fitted to 13 MIA (1 animal is missing data at 45 months) and 14 control animals and included fixed effects for group and time, with exchangeable within-animal covariance (except for lateral ventricles, for which spatial exponential covariance was used). One additional animal was excluded from the lateral ventricles model because of extreme data. Interactions between group and time were added to the models but were not retained in the reported models because the overall tests for time × group were not significant. The intercept can be interpreted as the predicted Time 1 volume (in mm³) for a Control animal.

Table 13. Parameter estimates from the unadjusted linear mixed-effects models for regional GM and WM volumetric measures[a]

	Frontal		Prefrontal		Cingulate		Temporal limbic	
Model term	Estimate (SE)	p	Estimate (SE)	p	Estimate (SE)	p	Estimate (SE)	p
GM volume								
Intercept	7380.2 (144.0)	<0.001	7070.3 (214.4)	<0.001	2314.1 (66.8)	<0.001	2430.7 (54.6)	<0.001
Difference (mm³) MIA vs Control	−564.6 (181.0)[b]	0.005[b]	−695.8 (319.5)[b]	0.039[b]	−161.3 (95.6)	0.10	−4.8 (78.1)	0.95
Difference (mm³) Time 2 vs Time 1	129.0 (49.0)	0.01	−43.2 (40.7)	0.30	3.7 (12.3)	0.77	258.6 (19.3)	<0.001
Difference (mm³) Time 3 vs Time 1	515.4 (64.7)	<0.001	14.4 (49.0)	0.77	1.4 (16.6)	0.93	545.8 (27.1)	<0.001
Difference (mm³) Time 4 vs Time 1	501.4 (52.8)	<0.001	−162.2 (51.6)	0.004	−52.5 (13.8)	0.001	561.3 (31.0)	<0.001
Difference (mm³) Time 5 vs Time 1	617.2 (68.2)	<0.001	−155.0 (48.5)	0.004	−41.7 (15.8)	0.014	601.5 (27.8)	<0.001
WM volume								
Intercept	2775.1 (85.0)	<0.001	1593.4 (59.5)	<0.001	350.6 (12.6)	<0.001	431.9 (11.8)	<0.001
Difference (mm³) MIA vs Control (at Time 1)	−187.3 (122.6)	0.14	89.8 (55.3)	0.12	2.0 (12.7)	0.88	7.5 (14.8)	0.62
Difference (mm³) Time 2 vs Time 1 (for Control)	377.1 (23.1)	<0.001	290.7 (15.0)	<0.001	32.7 (2.9)	<0.001	37.4 (3.2)	<0.001
Difference (mm³) Time 3 vs Time 1 (for Control)	907.0 (36.9)	<0.001	647.5 (25.2)	<0.001	93.6 (4.4)	<0.001	113.2 (5.0)	<0.001
Difference (mm³) Time 4 vs Time 1 (for Control)	1259.8 (45.5)	<0.001	838.9 (29.2)	<0.001	131.7 (5.2)	<0.001	143.6 (6.1)	<0.001
Difference (mm³) Time 5 vs Time 1 (for Control)	1540.1 (51.4)	<0.001	966.4 (34.5)	<0.001	154.1 (5.4)	<0.001	170.2 (5.8)	<0.001
Difference between groups in Time 2 vs Time 1 differences	−65.7 (33.2)	0.06	—		—		—	
Difference between groups in Time 3 vs Time 1 differences	−135.7 (53.1)	0.02	—		—		—	
Difference between groups in Time 4 vs Time 1 differences	−166.4 (65.6)	0.02	—		—		—	
Difference between groups in Time 5 vs Time 1 differences	−248.9 (74.9)	0.003	—		—		—	

[a]Time 1 = 6 months; Time 2 = 12 months; Time 3 = 24 months; Time 4 = 36 months; Time 5 = 45 months. Mixed-effects linear regression models were fitted to 13 MIA (1 missing at 45 months) and 14 control animals and included fixed effects for group, time, and their interaction, with unstructured covariance within animal. Interactions were not retained in the reported models if the overall test for time × group was nonsignificant. If the interaction is not included, the estimated difference between MIA versus Control is the same across time points, and the estimated difference between time points is the same within MIA and Control. If the interaction is included, difference between MIA versus Control is the estimated difference at Time 1 and the estimated differences between time points are for the Control. The intercept can be interpreted as the predicted volume (in mm³) at Time 1 for a Control animal.
[b]Statistically significant MIA versus Control group difference (p < 0.05).
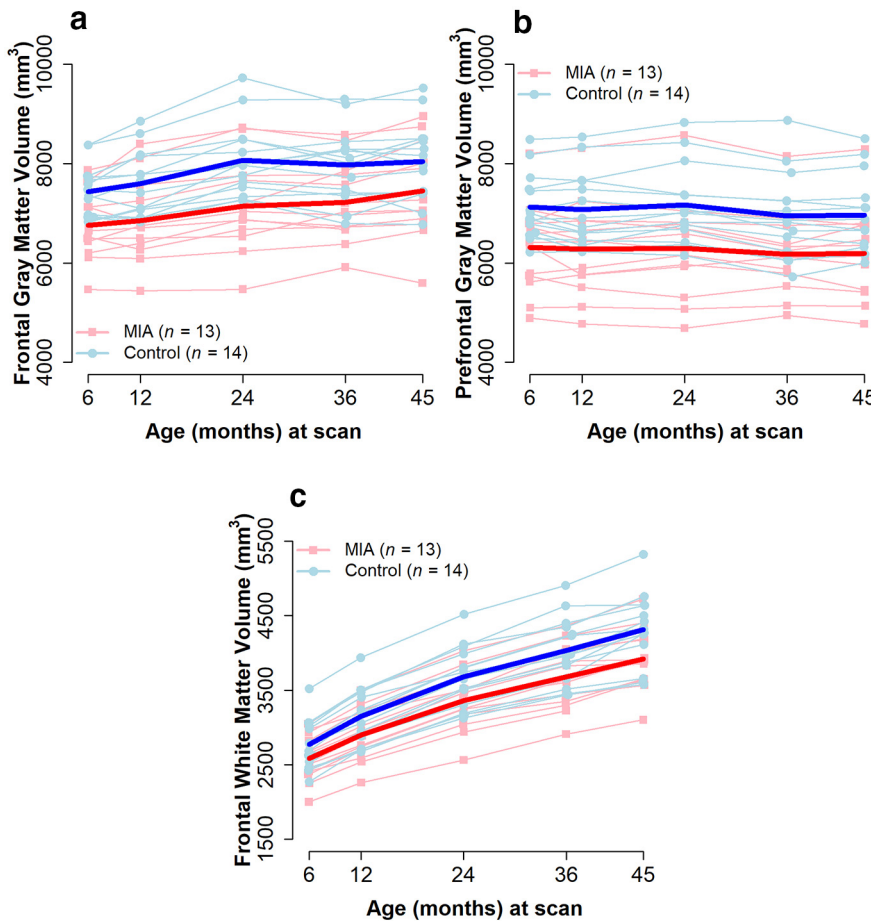
Figure 11. Brain volume trajectories for MIA-exposed and Control offspring for (**a**) GM frontal and (**b**) prefrontal regions, and (**c**) WM frontal region. Light lines indicate individual trajectories. Dark lines indicate average values for the two groups. GM group differences were significant in frontal and prefrontal regions, with lower volumes in MIA across all time points. For WM, group × time interaction was significant in the frontal region, with significantly smaller volume increases from the initial 6 month measurement to the 24, 36, and 45 month measurements in MIA relative to Control.

young adults diagnosed with SZ (Schwarz et al., 2019; Keshavan et al., 2020) and may serve as a biomarker of neurodevelopmental risk (Ursini et al., 2021).

Additional clinical and translational research is needed to understand how other factors, including genetic risk, gestational timing, nature and intensity of the maternal immune response, and additional postnatal events, determine which (if any) disease phenotype results from prenatal exposure to MIA. The vast majority of MIA models are conducted in rodents, although there is increasing interest in cross-species approaches using other species, including ferrets and pigs (Li et al., 2018; Rymut et al., 2020). Although the results of the present study extend the results of rodent MIA models into a species more closely related to humans, there are inherent logistic constraints to NHP studies. Limitations of the current study include a relatively modest sample size and exclusion of female offspring. We recognize that sex differences are emerging as a critical factor in MIA model studies (Coiro and Pollak, 2019) and will be focusing on the impact of MIA on the female NHP brain in our upcoming studies. As the NHP model requires 165 d gestation followed by 4 years of data acquisition, the complete characterization of offspring brain

Table 14. Parameter estimates from the linear mixed-effects models for gray and white ROI volumetric measures adjusted for total brain volume[a]

Model term	Frontal Estimate (SE)	p	Prefrontal Estimate (SE)	p	Cingulate Estimate (SE)	p	Temporal limbic Estimate (SE)	p
GM volume								
Intercept	7518.4 (95.9)	<0.001	7131.8 (101.5)	<0.001	2297.9 (26.6)	<0.001	2445.6 (28.0)	<0.001
Difference (mm³) MIA vs Control	−403.3 (140.9)[b]	0.01[b]	−387.6 (154.6)[b]	0.02[b]	0.9 (41.1)	0.98	82.2 (44.7)	0.08
Difference (mm³) Time 2 vs Time 1	−91.5 (31.9)	0.007	−257.5 (23.4)	<0.001	−59.5 (10.8)	<0.001	200.7 (16.1)	<0.001
Difference (mm³) Time 3 vs Time 1	−163.6 (57.2)	0.006	−645.5 (51.6)	<0.001	−193.2 (19.1)	<0.001	367.5 (25.9)	<0.001
Difference (mm³) Time 4 vs Time 1	−299.8 (58.9)	<0.001	−941.0 (64.7)	<0.001	−282.2 (22.1)	<0.001	350.8 (33.5)	<0.001
Difference (mm³) Time 5 vs Time 1	−410.9 (78.3)	<0.001	−1161.8 (74.3)	<0.001	−337.6 (27.3)	<0.001	329.3 (34.2)	<0.001
Brain volume (cm³)	93.3 (6.0)	<0.001	90.7 (5.6)	<0.001	26.7 (2.1)	<0.001	24.5 (2.4)	<0.001
WM volume								
Intercept	2775.1 (42.7)	<0.001	1656.1 (33.7)	<0.001	361.5 (8.3)	<0.001	441.6 (7.9)	<0.001
Difference (mm³) MIA vs Control (at Time 1)	−50.1 (63.4)	0.44	49.3 (44.1)	0.28	−4.4 (11.2)	0.70	9.2 (11.3)	0.42
Difference (mm³) Time 2 vs Time 1 (in Control)	303.4 (18.0)	<0.001	246.5 (12.0)	<0.001	24.7 (2.8)	<0.001	26.6 (3.0)	<0.001
Difference (mm³) Time 3 vs Time 1 (in Control)	676.6 (39.7)	<0.001	511.4 (24.9)	<0.001	68.8 (5.7)	<0.001	79.9 (5.3)	<0.001
Difference (mm³) Time 4 vs Time 1 (in Control)	1000.3 (46.3)	<0.001	678.4 (30.8)	<0.001	102.4 (6.8)	<0.001	104.3 (6.6)	<0.001
Difference (mm³) Time 5 vs Time 1 (in Control)	1207.2 (55.9)	<0.001	758.9 (37.0)	<0.001	116.2 (8.1)	<0.001	119.2 (7.4)	<0.001
Difference between groups in Time 2 vs Time 1 differences	−52.8 (23.1)	0.03	—	—	—	—	—	—
Difference between groups in Time 3 vs Time 1 differences	−88.9 (44.1)	0.06	—	—	—	—	—	—
Difference between groups in Time 4 vs Time 1 differences	−136.8 (52.3)	0.02	—	—	—	—	—	—
Difference between groups in Time 5 vs Time 1 differences	−214.0 (61.7)	0.002	—	—	—	—	—	—
Brain volume (cm³)	28.6 (3.2)	<0.001	18.7 (2.1)	<0.001	3.4 (0.6)	<0.001	4.6 (0.5)	<0.001

[a]Time 1 = 6 months; Time 2 = 12 months; Time 3 = 24 months; Time 4 = 36 months; Time 5 = 45 months. Mixed-effects linear regression models were fitted to 13 MIA (1 missing at 45 months) and 14 control animals and included fixed effects for group, time, and their interaction, brain volume, with unstructured covariance within animal. Interactions were not retained in the reported models if the overall test for time × group was nonsignificant. If the interaction is not included, the estimated difference between MIA versus Control is the same across time points, and the estimated difference between time points is the same within MIA and Control. If the interaction is included, difference between MIA versus Control is the estimated difference at Time 1 and the estimated differences between time points are for the Control group. Brain volume was lefted at 86,200; thus, the intercept can be interpreted as the predicted volume (in mm³) at Time 1 for a Control animal with a brain of 86,200 mm³. The estimate for brain volume can be interpreted as the average increase in ROI volume (in mm³) for a 1 cm³ increase in brain volume.
[b]Statistically significant MIA versus Control group difference (p < 0.05).

and behavioral development will require additional time for coding and analysis. However, the initial observation of reduced frontal GM and WM volume paired with subtle changes in cognitive development contributes to mounting evidence that early exposure to prenatal immune challenge triggers a pattern of divergent neurodevelopmental trajectories in MIA-treated offspring. Data collected from this unique NHP cohort will allow us next to explore behavioral, transcriptional, brain network, and immunologic profiles of MIA-treated offspring to better understand resilience and susceptibility to prenatal immune activation.

References

Barger N, Keiter J, Kreutz A, Krishnamurthy A, Weidenthaler C, Martinez-Cerdeno V, Tarantal AF, Noctor SC (2019) Microglia: an intrinsic component of the proliferative zones in the fetal rhesus monkey (*Macaca mulatta*). Cereb Cortex 29:2782–2796.

Bauman MD, Schumann CM (2018) Advances in nonhuman primate models of autism: integrating neuroscience and behavior. Exp Neurol 299:252–265.

Bauman MD, Lavenex P, Mason WA, Capitanio JP, Amaral DG (2004a) The development of mother-infant interactions after neonatal amygdala lesions in rhesus monkeys. J Neurosci 24:711–721.

Bauman MD, Lavenex P, Mason WA, Capitanio JP, Amaral DG (2004b) The development of social behavior following neonatal amygdala lesions in rhesus monkeys. J Cogn Neurosci 16:1388–1411.

Bauman MD, Iosif AM, Ashwood P, Braunschweig D, Lee A, Schumann CM, Van de Water J, Amaral DG (2013) Maternal antibodies from mothers of children with autism alter brain growth and social behavior development in the rhesus monkey. Transl Psychiatry 3:e278.

Bauman MD, Iosif AM, Smith SE, Bregere C, Amaral DG, Patterson PH (2014) Activation of the maternal immune system during pregnancy alters behavioral development of rhesus monkey offspring. Biol Psychiatry 75:332–341.

Bauman MD, Lesh TA, Rowland DJ, Schumann CM, Smucny J, Kukis DL, Cherry SR, McAllister AK, Carter CS (2019) Preliminary evidence of increased striatal dopamine in a nonhuman primate model of maternal immune activation. Transl Psychiatry 9:135.

Baxter MG, Gaffan D (2007) Asymmetry of attentional set in rhesus monkeys learning colour and shape discriminations. Q J Exp Psychol (Hove) 60:1–8.

Bergdolt L, Dunaevsky A (2019) Brain changes in a maternal immune activation model of neurodevelopmental brain disorders. Prog Neurobiol 175:1–19.

Brown AS, Meyer U (2018) Maternal immune activation and neuropsychiatric illness: a translational research perspective. Am J Psychiatry 175:1073–1083.

Careaga M, Murai T, Bauman MD (2017) Maternal immune activation and autism spectrum disorder: from rodents to nonhuman and human primates. Biol Psychiatry 81:391–401.

Cherel M, Budin F, Prastawa M, Gerig G, Lee K, Buss C, Lyall A, Consing KZ, Styner M (2015) Automatic tissue segmentation of neonate brain MR images with subject-specific atlases. Proc SPIE Int Soc Opt Eng 9413:941311.

Coiro P, Pollak DD (2019) Sex and gender bias in the experimental neurosciences: the case of the maternal immune activation model. Transl Psychiatry 9:90.

Crum WR, Sawiak SJ, Chege W, Cooper JD, Williams SC, Vernon AC (2017) Evolution of structural abnormalities in the rat brain following in utero exposure to maternal immune activation: a longitudinal in vivo MRI study. Brain Behav Immun 63:50–59.

Dettmer AM, Rosenberg KL, Suomi SJ, Meyer JS, Novak MA (2015) Associations between parity, hair hormone profiles during pregnancy and lactation, and infant development in rhesus monkeys (*Macaca mulatta*). PLoS One 10:e0131692.

Drazanova E, Ruda-Kucerova J, Kratka L, Horska K, Demlova R, Starcuk Z Jr, Kasparek T (2018) Poly(I:C) model of schizophrenia in rats induces sex-dependent functional brain changes detected by MRI that are not reversed by aripiprazole treatment. Brain Res Bull 137:146–155.

Estes ML, McAllister AK (2016) Maternal immune activation: implications for neuropsychiatric disorders. Science 353:772–777.

Giovanoli S, Notter T, Richetto J, Labouesse MA, Vuillermot S, Riva MA, Meyer U (2015) Late prenatal immune activation causes hippocampal deficits in the absence of persistent inflammation across aging. J Neuroinflammation 12:221.

Golub MS, Hogrefe CE, Germann SL, Tran TT, Beard JL, Crinella FM, Lonnerdal B (2005) Neurobehavioral evaluation of rhesus monkey infants fed cow's milk formula, soy formula, or soy formula with added manganese. Neurotoxicol Teratol 27:615–627.

Golub MS, Hogrefe CE, Vandevoort CA (2014) Binge drinking prior to pregnancy detection in a nonhuman primate: behavioral evaluation of offspring. Alcohol Clin Exp Res 38:551–556.

Golub MS, Hackett EP, Hogrefe CE, Leranth C, Elsworth JD, Roth RH (2017) Cognitive performance of juvenile monkeys after chronic fluoxetine treatment. Dev Cogn Neurosci 26:52–61.

Gordon JA (2019) A hypothesis-based approach: the use of animals in mental health research. National Institute of Mental Health Director's Message.

Guma E, Plitman E, Chakravarty MM (2019) The role of maternal immune activation in altering the neurodevelopmental trajectories of offspring: a translational review of neuroimaging studies with implications for autism spectrum disorder and schizophrenia. Neurosci Biobehav Rev 104:141–157.

Guo JY, Ragland JD, Carter CS (2019) Memory and cognition in schizophrenia. Mol Psychiatry 24:633–642.

Haddad FL, Patel SV, Schmid S (2020) Maternal immune activation by poly I:C as a preclinical model for neurodevelopmental disorders: a focus on autism and schizophrenia. Neurosci Biobehav Rev 113:546–567.

Izquierdo A, Jentsch JD (2012) Reversal learning as a measure of impulsive and compulsive behavior in addictions. Psychopharmacology (Berl) 219:607–620.

Kentner AC, Bilbo SD, Brown AS, Hsiao EY, McAllister AK, Meyer U, Pearce BD, Pletnikov MV, Yolken RH, Bauman MD (2019) Maternal immune activation: reporting guidelines to improve the rigor, reproducibility, and transparency of the model. Neuropsychopharmacology 44:245–258.

Keôpińska AP, Iyegbe CO, Vernon AC, Yolken R, Murray RM, Pollak TA (2020) Schizophrenia and influenza at the centenary of the 1918-1919 Spanish influenza pandemic: mechanisms of psychosis risk. Front Psychiatry 11:72.

Keshavan MS, Collin G, Guimond S, Kelly S, Prasad KM, Lizano P (2020) Neuroimaging in schizophrenia. Neuroimaging Clin North Am 30:73–83.

Knickmeyer RC, Styner M, Short SJ, Lubach GR, Kang C, Hamer R, Coe CL, Gilmore JH (2010) Maturational trajectories of cortical brain development through the pubertal transition: unique species and sex differences in the monkey revealed through structural magnetic resonance imaging. Cereb Cortex 20:1053–1063.

Knuesel I, Chicha L, Britschgi M, Schobel SA, Bodmer M, Hellings JA, Toovey S, Prinssen EP (2014) Maternal immune activation and abnormal brain development across CNS disorders. Nat Rev Neurol 10:643–660.

Li Y, Dugyala SR, Ptacek TS, Gilmore JH, Frohlich F (2018) Maternal immune activation alters adult behavior, gut microbiome and juvenile brain oscillations in ferrets. eNeuro 5:ENEURO.0313-18.2018.

Lyall AE, Woolson S, Wolfe HM, Goldman BD, Reznick JS, Hamer RM, Lin W, Styner M, Gerig G, Gilmore JH (2012) Prenatal isolated mild ventriculomegaly is associated with persistent ventricle enlargement at ages 1 and 2. Early Hum Dev 88:691–698.

Machado CJ, Whitaker AM, Smith SE, Patterson PH, Bauman MD (2015) Maternal immune activation in nonhuman primates alters social attention in juvenile offspring. Biol Psychiatry 77:823–832.

Malkova L, Heuer E, Saunders RC (2006) Longitudinal magnetic resonance imaging study of rhesus monkey brain development. Eur J Neurosci 24:3204–3212.

McCulloch CE, Searle SR, Neuhaus JM (2008) Generalized, linear, and mixed models. Hoboken, NJ: Wiley.

McCutcheon RA, Reis Marques T, Howes OD (2020) Schizophrenia: an overview. JAMA Psychiatry 77:201–210.

Meyer U (2019) Neurodevelopmental resilience and susceptibility to maternal immune activation. Trends Neurosci 42:793–806.

Meyer U, Feldon J (2010) Epidemiology-driven neurodevelopmental animal models of schizophrenia. Prog Neurobiol 90:285–326.

Meyer U, Schwendener S, Feldon J, Yee BK (2006) Prenatal and postnatal maternal contributions in the infection model of schizophrenia. Exp Brain Res 173:243–257.

Page NF, Gandal MJ, Estes ML, Cameron S, Buth J, Parhami S, Ramaswami G, Murray K, Amaral DG, Van de Water JA, Schumann CM, Carter CS, Bauman MD, McAllister AK, Geschwind DH (2021) Alterations in retro-transposition, synaptic connectivity, and myelination implicated by transcriptomic changes following maternal immune activation in nonhuman primates. Biol Psychiatry 89:896–910.

Piontkewitz Y, Arad M, Weiner I (2011) Abnormal trajectories of neurodevelopment and behavior following in utero insult in the rat. Biol Psychiatry 70:842–851.

Piontkewitz Y, Arad M, Weiner I (2012) Tracing the development of psychosis and its prevention: what can be learned from animal models. Neuropharmacology 62:1273–1289.

Rakic P (1988) Specification of cerebral cortical areas. Science 241:170–176.

Ramirez JS, Graham AM, Thompson JR, Zhu JY, Sturgeon D, Bagley JL, Thomas E, Papadakis S, Bah M, Perrone A, Earl E, Miranda-Dominguez O, Feczko E, Fombonne EJ, Amaral DG, Nigg JT, Sullivan EL, Fair DA (2020) Maternal interleukin-6 is associated with macaque offspring amygdala development and behavior. Cereb Cortex 30:1573–1585.

Rasmussen JM, Graham AM, Gyllenhammer LE, Entringer S, Chow DS, O'Connor TG, Fair DA, Wadhwa PD, Buss C (2021) Neuroanatomical correlates underlying the association between maternal interleukin-6 concentration during pregnancy and offspring fluid reasoning performance in early childhood. Biol Psychiatry Cogn Neurosci Neuroimaging Advance online publication. Retrieved Mar 23, 2021. doi: 10.1016/j.bpsc.2021.03.007.

Richetto J, Calabrese F, Riva MA, Meyer U (2014) Prenatal immune activation induces maturation-dependent alterations in the prefrontal GABAergic transcriptome. Schizophr Bull 40:351–361.

Rose DR, Careaga M, Van de Water J, McAllister K, Bauman MD, Ashwood P (2017) Long-term altered immune responses following fetal priming in a non-human primate model of maternal immune activation. Brain Behav Immun 63:60–70.

Rymut HE, Bolt CR, Caputo MP, Houser AK, Antonson AM, Zimmerman JD, Villamil MB, Southey BR, Rund LA, Johnson RW, Rodriguez-Zas SL (2020) Long-lasting impact of maternal immune activation and interaction with a second immune challenge on pig behavior. Front Vet Sci 7:561151.

Schepanski S, Buss C, Hanganu-Opatz IL, Arck PC (2018) Prenatal immune and endocrine modulators of offspring's brain development and cognitive functions later in life. Front Immunol 9:2186.

Schwarz E, Doan NT, Pergola G, Westlye LT, Kaufmann T, Wolfers T, Brecheisen R, Quarto T, Ing AJ, Di Carlo P, Gurholt TP, Harms RL, Noirhomme Q, Moberget T, Agartz I, Andreassen OA, Bellani M, Bertolino A, Blasi G, Brambilla P, et al. (2019) Reproducible grey matter patterns index a multivariate, global alteration of brain structure in schizophrenia and bipolar disorder. Transl Psychiatry 9:12.

Shi Y, Budin F, Yapuncich E, Rumple A, Young JT, Payne C, Zhang X, Hu X, Godfrey J, Howell B, Sanchez MM, Styner MA (2016) UNC-emory infant atlases for macaque brain image analysis: postnatal brain development through 12 months. Front Neurosci 10:617.

Short SJ, Lubach GR, Karasin AI, Olsen CW, Styner M, Knickmeyer RC, Gilmore JH, Coe CL (2010) Maternal influenza infection during pregnancy impacts postnatal brain development in the rhesus monkey. Biol Psychiatry 67:965–973.

Smith SE, Li J, Garbett K, Mirnics K, Patterson PH (2007) Maternal immune activation alters fetal brain development through interleukin-6. J Neurosci 27:10695–10702.

Testard C, Tremblay S, Platt M (2021) From the field to the lab and back: neuroethology of primate social behavior. Curr Opin Neurobiol 68:76–83.

Ursini G, Punzi G, Langworthy BW, Chen Q, Xia K, Cornea EA, Goldman BD, Styner MA, Knickmeyer RC, Gilmore JH, Weinberger DR (2021) Placental genomic risk scores and early neurodevelopmental outcomes. Proc Natl Acad Sci USA 118:e2019789118.

Vandeleest JJ, Capitanio JP, Hamel A, Meyer J, Novak M, Mendoza SP, McCowan B (2019) Social stability influences the association between adrenal responsiveness and hair cortisol concentrations in rhesus macaques. Psychoneuroendocrinology 100:164–171.

Vuillermot S, Joodmardi E, Perlmann T, Ogren SO, Feldon J, Meyer U (2012) Prenatal immune activation interacts with genetic Nurr1 deficiency in the development of attentional impairments. J Neurosci 32:436–451.

Wang J, Vachet C, Rumple A, Gouttard S, Ouziel C, Perrot E, Du G, Huang X, Gerig G, Styner M (2014) Multi-atlas segmentation of subcortical brain structures via the AutoSeg software pipeline. Front Neuroinform 8:7.

Weed MR, Bryant R, Perry S (2008) Cognitive development in macaques: attentional set-shifting in juvenile and adult rhesus monkeys. Neuroscience 157:22–28.

Weed MR, Taffe MA, Polis I, Roberts AC, Robbins TW, Koob GF, Bloom FE, Gold LH (1999) Performance norms for a rhesus monkey neuropsychological testing battery: acquisition and long-term performance. Brain Res Cogn Brain Res 8:185–201.

Weir RK, Forghany R, Smith SE, Patterson PH, McAllister AK, Schumann CM, Bauman MD (2015) Preliminary evidence of neuropathology in nonhuman primates prenatally exposed to maternal immune activation. Brain Behav Immun 48:139–146.

Willette AA, Lubach GR, Knickmeyer RC, Short SJ, Styner M, Gilmore JH, Coe CL (2011) Brain enlargement and increased behavioral and cytokine reactivity in infant monkeys following acute prenatal endotoxemia. Behav Brain Res 219:108–115.

Yushkevich PA, Piven J, Hazlett HC, Smith RG, Ho S, Gee JC, Gerig G (2006) User-guided 3D active contour segmentation of anatomical structures: significantly improved efficiency and reliability. Neuroimage 31:1116–1128.